

ADHESION STUDIES WITH ULTRA-THIN GLASS

BY

CURTIS FEKETY

A THESIS

SUBMITTED TO THE FACULTY OF

ALFRED UNIVERSITY

IN PARTIAL FULFILLMENT OF THE REQUIREMENTS
FOR THE DEGREE OF

MASTER OF SCIENCE

IN

GLASS SCIENCE

ALFRED, NEW YORK

February, 2022

ADHESION STUDIES WITH ULTRA-THIN GLASS

BY

CURTIS FEKETY

B.S. CHEM, MANSFIELD UNIVERSITY (1995)

SIGNATURE OF AUTHOR _____

APPROVED BY _____

Dr. WILLIAM LACOURSE, ADVISOR

Dr. S.K. SUNDARAM, ADVISORY COMMITTEE

Dr. ALEXIS CLARE, ADVISORY COMMITTEE

Dr. DORIS MONCKE, CHAIR, ORAL THESIS DEFENSE

ACCEPTED BY _____

GABRIELLE G. GAUSTAD, DEAN
KAZUO INAMORI SCHOOL OF ENGINEERING

Alfred University theses are copyright protected and may be used for education or personal research only. Reproduction or distribution in part or whole is prohibited without written permission from the author.

Signature page may be viewed at Scholes Library, New York State College of Ceramics, Alfred University, Alfred, New York.

ACKNOWLEDGMENTS

I would first like to thank my professor and advisor, Dr. William LaCourse, as well as the other excellent faculty and staff at Alfred University whom I have encountered, including my talented professors Dr. Roger Loucks, Dr. William Carty, Dr. Scott Misture, Dr. Kun Wang, committee members Dr. S.K. Sundaram, and Dr. Alexis Clare, as well as Dr. Darren Stohr for advice and reviewing my thesis progress, and Ms. Emilie Carney for always finding answers whenever I had procedural questions.

In addition, I must thank a large number of individuals at Corning Incorporated for their support, including my supervisor Mr. Paul Johnson, and Director Dr. Butchi Vaddi as my advocates to begin this adventure and providing for this great opportunity. I would also like to thank Dr. Todd St. Clair, Dr. Prantik Mazumder, and Dr. Arlin Weikel for both advice and support by allowing me use of certain lab resources and reference materials. I also received direct help and instruction at various points from a multitude of lab personnel including, in no particular order, Ms. Brandy Fuller, Ms. Angela Vaughn, Mr. Christopher Drake, Mr. Dennis Post, Mr. Kevin McCarthy, Ms. Diane Guilfoyle, Mr. Jerry Zhou, and Mr. Thomas Garvey. And I offer a special thanks to Dr. John Wight for his constant curiosity, enthusiasm, and encouragement as a colleague and AU alumni.

Lastly, I especially need to thank my wife, daughter, and extended family for enduring this challenge with me as a mid-career student. Between the stress of juggling classes, working full time, and trying to carve out moments for family, as well as the unexpected and manifold effects of COVID-19 on all of our lives, there were many moments where I was not my “best self”. I humbly appreciate their constant support and making time and space to help me achieve this goal.

TABLE OF CONTENTS

	Page
<i>Acknowledgments</i>	<i>iii</i>
<i>Table of Contents</i>	<i>iv</i>
<i>List of Tables</i>	<i>vi</i>
<i>List of Figures</i>	<i>vii</i>
<i>Abstract</i>	<i>ix</i>
I. INTRODUCTION	1
A. BACKGROUND ON ADHESION SCIENCE.....	4
1. <i>Electrostatic</i>	5
2. <i>Mechanical Interlocking</i>	6
3. <i>Chemical Bonding and Diffusion</i>	6
4. <i>Physical Adsorption (Surface Energy)</i>	7
II. EXPERIMENTAL	9
A. MATERIALS AND METHODS:.....	9
1. <i>Fusion Draw</i> –.....	9
2. <i>Sheet Redraw</i> –.....	10
3. <i>Folded Glass Samples</i> –.....	11
4. <i>Contact Angle</i> –.....	12
5. <i>Wedge Test</i> –.....	14
6. <i>Peel Tests</i> –.....	15
B. EXPERIMENTAL PROCEDURES:.....	16
1. <i>Sample Preparation</i> –.....	16
2. <i>Contact angle</i> –.....	17
3. <i>T-Peel Tests</i> –.....	17
4. <i>90° and 180° Peel Tests</i> –.....	18
5. <i>Surface Treatments</i> –.....	19
III. RESULTS AND DISCUSSION	20
1. <i>SFE by Contact Angle</i> –.....	20
2. <i>SFE by Wedge Test</i> –.....	21
3. <i>Pellicle T-Peel</i> –.....	22
4. <i>Film / Tape Tests</i> –.....	24

5.	<i>Film / Tape Tests</i> –.....	27
6.	<i>Elastic / Plastic Effects</i> –.....	30
IV.	SUMMARY AND CONCLUSIONS	33
V.	REFERENCES	35
VI.	APPENDIX	38

LIST OF TABLES

	Page
Table I – Surface Free Energies of Various Glass Samples, calculated via Contact Angle measurements using OWRK method.....	19
Table II - Surface Free Energies of Pellicle Samples via Wedge Test.....	20
Table III - Average Peel Strengths of Cling Film at Various Conditions.....	26
Table IV - Average Peel Strengths of Frisket Film at Various Conditions.....	27
Table V - Average Peel Strengths of Blue Tape at Various Conditions.....	27
Table VI - Average Peel Strengths of Red Tape at Various Conditions.....	27
Table VII - Max - Min Values of Critical Thickness vs. Actual.....	29
Table VIII - Normalized Values Extrapolated from Universal Peel Diagram.....	31

LIST OF FIGURES

	Page
Figure 1. Diagram of Fusion Glass Forming Process	8
Figure 2. Folding Glass to Form a Pellicle.....	10
Figure 3. Comparison of Pellicles, Fresh vs. Briefly Packaged.	11
Figure 4. Diagram of Droplet Contact Angle	12
Figure 5. Example of High vs. Low Contact Angle.	13
Figure 6. Diagram of Wedge Test.	13
Figure 7. Imass SP-2100 Peel Test Instrument.....	14
Figure 8. 90° Peel Test with Blue Tape.	17
Figure 9. T-Peel of Pellicles, 50um (Left) and 35um (Right).	20
Figure 10. Measured T-Peel Strength with 50-micron Pellicles.	21
Figure 11. Measured T-Peel Strength with 35-micron Pellicles.	21
Figure 12. Adhesive Failure Points Without Pre-Crack.	22
Figure 13. Peel Strength of Various Adherends on Fresh Sample.....	23
Figure 14. Peel Strength of Four Tapes on Sister Samples At Various Speeds.....	24
Figure 15. Adhesive Stringing from Red Tape.	25
Figure 16. Schematic of 90° Peel, Segmented into Elastic and Plastic Effects.....	29
Figure 17. Universal Peel Diagram Extrapolated from Kim's Original.....	30

ABSTRACT

A phenomenon was observed during work producing “ultra-thin glass” (<150 μ thickness) where samples folded onto themselves displayed strong adhesion and served as a simple method to analyze contaminants in the process and packaging of resulting ware. Subsequent Contact Angle, Wedge Test, and T-Peel studies were performed to understand the baseline of Surface Free Energy (SFE) for this direct bonding and attempts were made to refresh aged and packaged samples through various cleaning steps to produce a similar effect. When results showed SFE change was minimal between aged, cleaned, and fresh glass and no treatments enabled similar direct bonding to fresh samples, 90° and 180° Peel Test with adhesive tapes and films were used as a surrogate to rank the effectiveness of attempted cleaning procedures. Such tests yielded widely ranging values inherent to known issues with peel testing, but provided useful data to calculate true adhesion values of just 2 – 2.5 N/m, which were 1 to 3 orders of magnitude less than the experimental values due to work absorbed by elastic/plastic effects when peeling the polymer adherend. Highly flexible glass samples do not experience plastic deformation, so studying direct bonded ultra-thin glass provides a unique perspective on adhesion studies by excluding plastic effects. It was also demonstrated that although the direct bonded samples had even lower peel strengths after initial separation, the bond strength was higher than strong tapes and even epoxy prior to edge-crack formation, showing the usefulness of direct bonding in optical materials and potential for future development.

I. INTRODUCTION

Over the past 5,000+ years of human civilization¹, glass has been used in making containers, trade currency, ornamental jewelry, windows, lenses, modern scientific instrumentation, and electronic displays of all sorts. However, even the most impressive glass is obviously not without material limitations, such as fragility. Modern glass products include laminate materials with various organic and inorganic coatings used to modify toughness or durability of many consumer products such as bottles, smartphone screens, automobile windshields, optical fiber, and many more². In each case, a specific set of properties or enhancements is achieved by the combination of glass and one or more materials. A large portion of such applications involve use of polymeric coatings or films. A classic example is the automobile windshield, where a laminate of glass and soft polymer has become the global standard, preventing injury from flying glass shards during a collision or ejection from the vehicle by deforming to absorb impact energy, maintaining overall shape integrity, and retaining the broken glass thanks to its polymeric layer³.

Other examples⁴ of the usefulness of glass-polymer composites include various containers, which can have a thick soft coating to prevent leakage of hazardous liquids in case of breakage, or a thin lubricious coating to prevent frictional damage when rubbing together during processing. Windows and display screens are often covered in a polymer film for protection from damage and dust during shipping and handling. Eyeglasses can be augmented with anti-reflective, scratch-resistant, and photochromic coatings. Polymer films are very commonly applied by the consumer onto smartphone screens as a sacrificial layer to prevent damage to the display glass.

A particularly interesting example features glass cellphone screen protectors which are commonly tempered glass, although chemically strengthened glass versions are also available, which provide a more scratch resistant, but still sacrificial, layer of protection for the original device screen. A forceful drop or other impact may cause the catastrophic

fracture of a glass screen protector, yet the underlying original screen remains unharmed. Perhaps surprisingly, the relatively weak adhesion provided by a transparent silicone adhesive⁵ has a distinct advantage here in that it encourages lateral dissipation of energy, which discourages crack propagation from one glass layer to the next and protects the device.

While the benefits of polymeric coatings in each of these cases may be obvious, the role of adhesion is less intuitive, and must run a gamut of strengths, dependent on the application. The coating on a medical vial requires much stronger adhesion than the screen protector on a cellphone, for example, or it could peel away or lift off in limited areas. Even if it was effective at preventing damage, it would reduce consumer confidence in the product, perhaps leading to a waste of valuable doses of medicine or vaccine. In the reverse case, consumers would be quite hesitant to cover their phone display with a permanently bonded film, for fear of misalignment, trapped bubbles, etc.

The relative strength of adhesion between glass and an adjacent layer of material (polymer, glass, inorganic coating, etc.) must be carefully engineered to suit its application and optimized to deliver the desired composite features while avoiding negative (real or perceived) side effects. Very often, a strong or “permanent” bond is needed to prevent delamination and a polymeric coating is directly applied to the glass via liquid or vapor phase processes and generally employs a chemical “adhesion promoter” such as an organosilane⁶. Alternatively, a solid-phase layer (glass, film, substrate) may be applied either directly, or using liquid-phase adhesive, to form a strongly bonded composite material.

There are also numerous applications where a weaker bond is beneficial. Here, a liquid-phase adhesive may be used, as in most tapes which use a Pressure-Sensitive Adhesive (PSA). This can also be achieved using a polymer (or glass) with no discernible adhesive tack at all, such as when putting a screen protector on a display or cling-wrap over a glass dish. Applications also exist where the risk of residue or contamination may restrict the use of liquid-phase adhesives, such as packaging films used in shipping windows,

doors, electronic devices, optical lenses, and the materials used in manufacturing them, such as large sheets of display glass. In such cases, the system must provide sufficient adhesion to keep the film in place, while remaining easy to peel off, and guarantee any adhesive or contaminants present stays with the film upon removal.

The work detailed herein deals with adhesion on “Ultra-thin” glass sheets (≤ 150 -micron thicknesses) which have earned considerable interest over the past decade due to a somewhat remarkable property of flexibility added to the normal benefits of glass materials. Numerous potential uses include bendable displays for cellphones, tablets, and wearable electronic devices, protective light-weight coverings for solar panels, and durable skins for home and office products, such as whiteboards, countertops, and such. It also provides a unique opportunity for a fundamental study of glass to glass adhesion, which could provide insights into the intriguing “dark art” of Direct Bonding⁷.

Direct Bonding, also known as Optical Contacting, has been shown to give “weak” bonding between two highly polished and pristine glass surfaces without any need for an adhesive layer. This phenomenon was notably studied by both Newton and Rayleigh. An adaptation of the adhesive-less metal bonding technique known as “*Anspergen*” (jumping together) was used by German artisans for many years in fabrication of precision prisms before it found more widespread usefulness in silicon wafer processing⁸. Modern developments have added solution processing to enable improved alignment and chemically activated surfaces for stronger bonding, while retaining the advantages of eliminating optical losses and thermal effects derived from using an adhesive layer between glass surfaces.

It was observed that Direct Bonding often occurs between two freshly created glass surfaces, given that they are flat and clean enough, and is often observed when working with ultra-thin glass production. These surfaces seem to be attractive not only to each other, but also to any nearby contaminants, which reduce surface energy and physically interfere with direct bonding. Nonetheless, techniques to create direct bonding may present

opportunities for developing scientifically interesting and novel laminate structures of ultra-thin materials in the near future.

A. Background on Adhesion Science

The IUPAC definition of Adhesion is the:

“Process of attachment of a substance to the surface of another substance.”

(Note: Adhesion requires energy that can come from chemical and/or physical linkages, the latter being reversible when enough energy is applied.)

This differs from “cohesion” (the forces holding a single phase, or “similar”, matter together) in that adhesion figures in causing two or more material phases to stick together. It can be argued⁹ that these fundamental forces are practically one and the same, the major difference being that Adhesion involves two “dissimilar” materials and their surfaces. This means that other factors may come into play, such as CTE mismatch, distance between the surfaces, and any foreign agents which might interfere with the contact of the surfaces.

Abbott¹⁰ and others describe a relatively small number of ways that adhesion can occur, although views may differ on their order of importance:

1. Electrostatic
2. Mechanical Interlocking
3. Chemical Bonding
4. Diffusion (Intermingling / Entanglement)
5. Surface Energy

For the purposes of studying useful glass-to-glass direct bonding and adhesive bonding of polymeric materials on glasses, Electrostatic and Mechanical Interlocking can be considered out of scope for this study. This is not meant to suggest these modes are not

worthy of consideration in their proper place, and each must be understood and either used or avoided in any number of controlled industrial settings. Chemical Bonding and Diffusion are extremely important when considering functionally enhanced Direct Bonding of glass surfaces, as well as in other cases, and certainly merits discussion, even if only as a counterpoint to this research. Therefore, from a practical standpoint, this work will focus primarily on the effects of “physical” treatments of the glass surface, as opposed to the more common “chemical” treatments, which will be described later. As justification for this focus, a few pertinent examples may be in order.

1. Electrostatic

Electrostatic forces are well known for the ability to attract and hold two materials together, at least temporarily, depending on factors such as mass and surface charge. This can be readily observed by holding a balloon to a wall after being triboelectrically charged from rubbing against one’s hair, capturing dust particles from surfaces with a feather duster, and removing pollutants from room air onto charged collecting plates in electronic air purifiers. As was highlighted during the outset of the COVID-19 pandemic, electrostatic charges are also used to greatly enhance the efficacy of N95-type masks, but this transient gain is limited to a single use, which contributed to global mask shortages in early 2020¹¹. Such effects are notably problematic for glass manufacturing, where static charge can build up on glassware due to ionization as it is processed, or from triboelectric charging as it is transported. This can cause dust particles to adhere to the glass surface strongly enough to avoid easy removal, and is generally to be avoided at considerable engineering and equipment cost by minimizing particulate in the production environment, neutralizing charge on the glass with de-ionizers, and swift application of protective film, such as Visqueen (polyethylene).

If the particles are very small, as in certain oxide nanoparticles, this effect can be so strong that a cohesive layer several millimeters thick can adhere to a statically-charged glass surface not only overcoming gravity, but fluidly passing over a rod scraped along the surface to reattach to the glass on the opposite side¹². However, even this strong electrostatic effect is merely temporary, as it will dissipate over time at some rate dependent

on humidity, wettability, and dielectric properties of the materials¹³. The electrostatic charge may take seconds or days to bleed off, but it will eventually happen, and take its adhesive force with it, therefore we cannot count on electrostatics for long-term adhesion applications.

2. Mechanical Interlocking

Mechanical Interlocking involves the flow of liquid-phase adhesive into the pore structure of a substrate, or “adherend”, where it then solidifies via curing, evaporation, or cooling. This physical interlocking anchors the adhesive into the substrate, increases surface area, and the convoluted path may disrupt crack propagation. This effect can lead to excellent bonding, approaching or exceeding cohesive strength, but does require a porous substrate or a carefully engineered surface structure. As almost all relevant glass products lack these structures since it would interfere with optical transparency, this type of adhesion deserves little consideration here.

Although one could consider specialized glasses such as porous Vycor¹⁴ which might allow an adhesive to penetrate its structure. Porous Vycor is made by re-heating an alkali-borosilicate glass so that it phase-separates into a silica-rich phase and an alkali-boron rich phase, which is soluble in acid. On soaking in an acid solution, the alkaline-rich phase dissolves, leaving behind a complex pore structure within the surviving borosilicate glass, which could be penetrated by a liquid adhesive. Some other approaches to create a complex topography on a normally flat glass surface include laser damaging, perforation, selective etching, or combinations thereof. In any case, these can be considered niche areas of glass manufacturing compared to most commercial applications.

3. Chemical Bonding and Diffusion

Chemical Bonding and Diffusion can be considered together to some degree in that they involve molecular bonds spanning from the adhesive material into the chemical structure of the adherend, or vice versa. The bonds can be simple linear bonds to Si-O-H groups on the glass surface, for example, or more complex or “entangled” polymeric bonds

achieved by using an adhesion promoter (i.e. a fluorosilane or silicone) compound mixed into the adhesive or applied as a primer layer. This can also be done with an inorganic primer, such as SnO₂ “hot-end coating”, which provides a well-bonded anchor layer for a lubricious “cold-end coating” in the bottling industry¹⁵ that enables high-speed processing while minimizing breakage. More recently, these methods have also been employed to enhance the strength of direct bonding or to provide some level of crack protection at the joint. Diffusion behaves similarly through kinetic rather than chemical means, carried out over a longer time scale or at high temperature, where molecules of one material intermingle with the other to some depth of penetration and are not easily pulled apart. This results in an essentially continuous material where some compositional gradient, but no obvious interface can be found in a cross-section of the bonded area.

These types of adhesive bonding can give excellent strength and are often used throughout research and industry. However, processing of these adhesives and primers tends to be complicated, with a very large number of factors at play, and could entail a lifetime of study for just a small fraction of available systems. Nonetheless, a well-understood adhesive system of this kind can be tuned, via concentration and type of adhesion promoter as well as processing and curing conditions, such that adhesion strength is controllable and optimized for a given application.

4. Surface Energy

This leaves us with the consideration of adhesion caused by surface energy such as physical adsorption. This type of adhesion depends on attractive Van der Waals forces which exist between all matter at atomic scale distances and does not require presence of any additional adhesive layer or the system is designed to fail with the adhesive strongly attached to the adherend. Many products make use of relatively low-strength adhesion, for instance cling wrap, Visqueen film, and cellphone screen protectors, to name a few. The surface energy effect is most utilized in the area of “Direct Bonding”, where silicon wafers and ultra-thin glass pieces are temporarily attached to a more robust carrier substrate to enable mechanical processing without breakage, yet the risk of residue is simply too great to allow use of any adhesive at all¹⁶.

Direct Bonding between two glasses can also be converted to a permanent bond under proper conditions of time and temperature by conversion of the relatively weak Si-O-H hydrogen bonding on either surface to much stronger covalent Si-O-Si bonds. This fascinating bridge into the realm of chemical bonding and diffusion has been known for well over a century but somewhat neglected today and is even described as a “Dark Art” by noted practitioner Vaz Zastera and others, as referenced previously. His recent work in silica glass sculpture and lens engineering demonstrates that with great care and skill this form of adhesion has strength which competes with the cohesive forces in the individual pieces. Many commercial glasses also contain various dopant ions at or near the glass surface which may allow moderately strong ionic bonds to form at the interface.

The role of surface energy is important in the function of adhesive tapes and films, in that it determines the wettability of a liquid-phase adhesive to the glass surface. The effect is easily demonstrated by applying a drop of liquid adhesive to a low-energy (“dirty”) versus a high-energy (“clean”) glass sample and observing the contact angle. If the droplet spreads readily, it lowers the surface energy via strong interactions with the substrate surface. If it remains as a ball or hemisphere, there is little interaction or bonding with the substrate. Although this seems obvious and something which most scientists “know”, there is actually considerable debate in the field of Adhesion Science on the real impact of surface energy. Developers of adhesives, known as “Formulators”, commonly pursue increased surface energy and report higher adhesion strengths to varied degree, and conclusions seem to run the gamut of “surface energy is everything” in regards to clean surfaces, to “surface energy is almost negligible”¹⁷ when considering the relatively small contribution of SFE compared to the observed peel strength of a PSA. One colleague colorfully described the relationship of adhesion strength to surface energy by analogy of correlating successful marriages to successful first dates, in that “you cannot have one without the other, but after that the correlation drops off”¹⁸. The following work will attempt to use the platform of ultra-thin glass to shed light on this confusing situation.

II. EXPERIMENTAL

A. Materials and Methods:

1. Fusion Draw –

At this point, the “Fusion Process” invented by Corning Incorporated¹⁹ in the 1960’s is relatively well-known in technical and popular technological literature as a preeminent manufacturing process for glass sheets used in flat-screen televisions, laptop computers, and hand-held electronic devices. The heart of this process is a specially engineered trough known as an “Isopipe” which is filled with molten glass until it overflows on both faces (Fig. 1). As the molten glass flows down the faces and reached the bottom of the trough, the two streams join and form a single sheet with the outside surfaces that have never contacted anything other than air. As the molten glass begins to solidify after fusing together, the sheet is pulled downward from the edges, which are subsequently cut off, leaving a glass sheet with pristine surfaces.

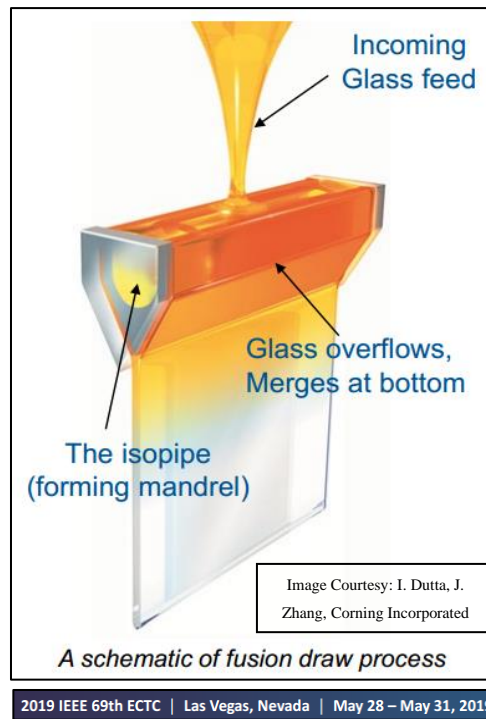


Figure 1 – Diagram of Fusion Glass Forming Process

This manufacturing process has a distinct advantage of excellent surface flatness and low thickness variation, which is necessary for the study of adhesion and surface energy, and all glass source material used in this study originated from the Fusion Draw process.

2. Sheet Redraw –

A second Corning process²⁰ known as “Glass Sheet Redraw” was used to reduce the thickness of the original Fusion-formed glass sheets from >1000 microns to <150 microns, while maintaining approximately the incoming width, therefore the length extends in proportion to the thickness reduction or “Redraw Ratio”. For example, reducing the thickness of a 1000 micron incoming sheet to 100 micron output gives a Redraw Ratio of 10, so 100 cm of glass yields roughly 1 meter of Ultra-Thin Glass (UTG) with a resultant ~10X increase in surface area, meaning a lot of new surface is created. The Redraw process is carried out by inserting a relatively thick sheet of source glass centered in a vertical furnace chamber and heated to an appropriate temperature for the glass to be formable, usually in the neighborhood of 10^6 Poise.

The viscous glass sheet forms a gob which sags somewhat faster than the sheet is driven through the furnace until it can be contacted by motorized wheels near the edge of the sheet, much like in the Fusion process, and the glass is stretched to the desired thickness. The entire process of heating the sheet to near the softening point and stretching it essentially resets the original surface to a clean and dry high-energy state which is comingled with newly created surface. Once again, the parts in contact with any other surface are cut off, resulting in a thinner version of the incoming sheet from which samples were harvested, and the original surface quality is maintained, allowing it to be used for our adhesion studies. In addition to the excellent surface flatness and pristine state, the thinned glass provided an opportunity to study glass to glass adhesion (Direct Bonding), as will be mentioned later. One caveat worth noting is that all glass samples were harvested from the interior of the redrawn sheet by diamond-scribing and snapping, which certainly

left damage and debris at the edges, but was thought preferable to more intense action of a diamond saw or thermal effects from laser-cutting.

5. Folded Glass Samples –

At thicknesses below ~150 microns, glass begins to become flexible, which seems remarkable at first glance, but as has been pointed out by numerous experts, any material becomes flexible at sufficiently low thicknesses²¹. In glass, this can be impacted by use of various network modifiers and process conditions to enhance the native flexibility while maintaining other desirable properties such as scratch resistance to make useful products such as Corning’s Willow glass.

For these experiments, a commercial version of Corning Gorilla glass was used, and its excellent bendability at thicknesses of 100 microns and below enabled folded samples, called glass “Pellicles” (Fig. 2), to be made immediately upon exiting the redraw process, while the glass was still very warm, dry, and clean. Such pellicle samples have previously been used to demonstrate cleanliness at the redraw process outlet versus progressive contamination through subsequent handling steps, and optical analysis of glass pellicles are a well-known tool to study environmental particulate²².

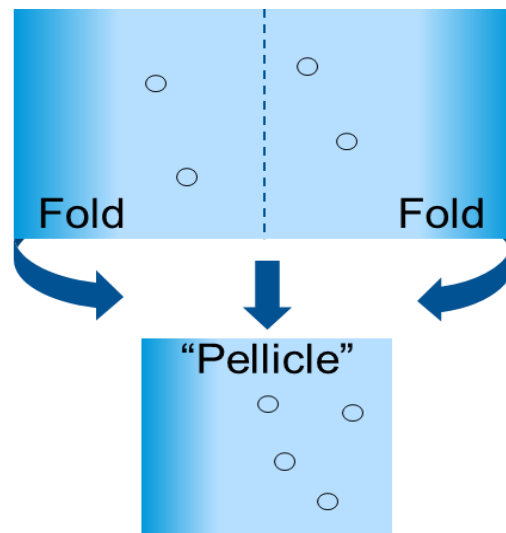


Figure 2 - Folding Glass to Form a Pellicle

The function of this is simple and traces all the way back to Newton's investigations on adhesion between glass surfaces and the so-called "Newton's Rings" which are defined by the separation distance radiating from a point of adhesive contact²³. With pellicle samples, bubbles are somewhat analogous to rings in that they give information regarding the separation distance wherever adhesion is prevented by presence of a film or debris, trapped gas, or a general loss of surface energy due to hydration or oxidation. The size of the bubble is always somewhat larger than the contaminant, and loosely correlates to the area and height of the foreign matter for a given thickness and modulus of pellicle material as it deforms around the debris.

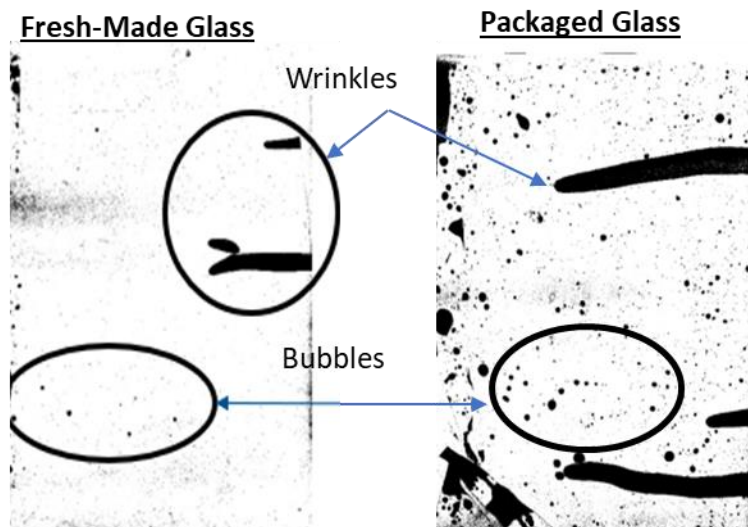


Figure 3 - Comparison of Pellicles, Fresh vs. Briefly Packaged

The present study uses these glass pellicle samples in studying surface free energy (SFE) and adhesion by performing Wedge and T-Peel tests on 1" wide strips carefully harvested from larger pellicles. This data was also compared to SFE results on glass at various times after emerging from the redraw process.

6. Contact Angle –

Surface Free Energy was calculated in the Krüss Advance software by the Owens, Wendt, Rabel and Kaelble (OWRK) method²⁴ using Contact Angle measurements

performed with a Krüss Mobile Surface Analyzer (MSA) meter with de-ionized water and Diiodomethane as polar and non-polar liquids, respectively.

The OWRK method entails use of Young's equation (Eq. 1), to calculate the SFE of a solid, σ_s , from the interfacial tension between solid and liquid, σ_{sl} , Surface tension of the liquid, σ_l , and Contact Angle of the droplet, θ .

$$\sigma_s = \sigma_{sl} + \sigma_l \cdot \cos\theta \quad (1)$$

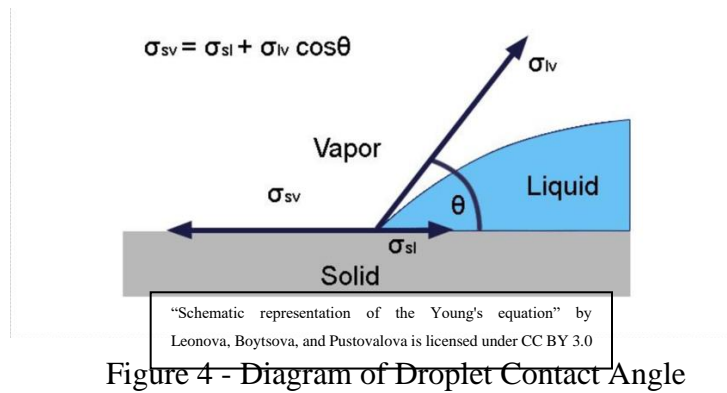


Figure 4 - Diagram of Droplet Contact Angle

Since σ_{sl} is unknown, it must be calculated using Fowkes' method (Eq. 2) by assessing the contributions of the polar (P) and disperse (D) portions of the solid phase by using two liquids, one polar and one non-polar, as wettability is proportional to the match between solid and liquid polarity.

$$\sigma_{sl} = \sigma_s + \sigma_l - 2(\sqrt{\sigma_s^D \cdot \sigma_l^D} + \sqrt{\sigma_s^P \cdot \sigma_l^P}) \quad (2)$$

The baseline results were verified using a larger, stationary instrument (Krüss model DSA 100E), but the handheld unit was far preferable for its portability and speed – allowing for nearly immediate measurement of samples after exiting redraw, and customizability of droplet size and imaging time which allowed rapid capture of water droplet contact angle on freshly made samples, which was not possible with the larger system. This was necessary due to the extremely high wetting of the water droplets on all

but the oldest, non-cleaned samples where water CA was less than 10 degrees, however diiodomethane did not have any difficulty in reading on either system.



Figure 5 - Example of High vs. Low Contact Angle

That said, there was clearly an effect of time in ambient atmosphere, as it was only possible to make well-adhered pellicles within moments of exiting the redraw process, after which adhesion degraded to nil within minutes of exposure to room air or immediately after exposure to packaging surfaces, probably due to adsorbed water or organic vapors and particulate contamination over the entire surface. However, the difference of SFE measured by this method from fresh to aged samples remained quite small, and it is difficult to imagine this being responsible for the observed dramatic drop in adhesion of pellicles on anything other than fresh-made glass which was mere moments old.

7. Wedge Test –

Another method to assess the SFE and adhesion between the glass surfaces of pellicle samples was the “Wedge Test”, as described by Maurel-Pantel et al.²⁵ in which a 1” wide strip was harvested from a bubble-free area of a pellicle. A fresh razor blade of a given thickness was inserted into a point of separation, usually at a corner, and the blade

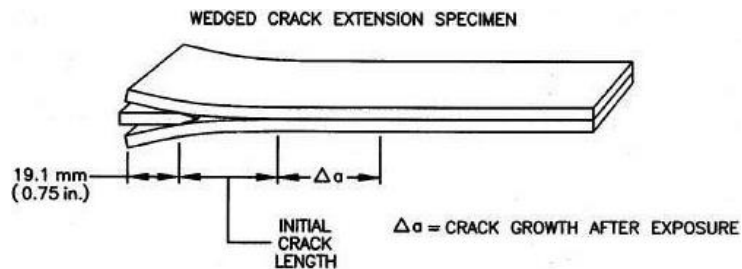


Image Courtesy: <https://www.testresources.net/images/accessories/standards-fixturing/gd3762-99-014-astm-d3762-test-fixture-1.jpg>

Figure 6 - Diagram of Wedge Test

was slowly worked inwards to form a separation front parallel to the leading edge of the razor blade.

The entire setup is then placed under a microscope and progression of the separation front is measured over a set amount of time, and the distance from the blade edge to the front is recorded and used to calculate the Bonding Energy, W , in Joules/square meter which is approximately equal to the Critical Strain Energy Release Rate, G_c , per eq. (3):

$$G_C = \frac{3Et^3y^2}{16L^4} = W = 2\gamma \quad (3)$$

where E is the Young's Modulus of the glass in Pascals, t is the thickness of glass sheet in meters, y is the thickness of the razor blade in meters, and L is the "crack length" measured from the forward edge of the razor blade to the separation front. The estimated Bonding Energy can then be halved to give the approximate Surface Energy in Newtons/meter since the two bonding surfaces are assumed to be identical in this case and given that 1 J/m^2 is equivalent to 1 N/m .

8. Peel Tests –

The other important analytical method used for this study was the "Peel Test" performed at 90° , 180° , and in a "T-Peel" fashion using an Imass SP-2100 unit.



Figure 7 - Imass SP-2100 Peel Test Instrument

The T-Peel tests run on 50-micron pellicle samples showed stable results, but absolute values may be skewed due to bending angle and modulus of the glass, requiring some correction factor in order to be useful, while tests on any thicker samples resulted in

subject failure of the glass. Since peel testing of pellicle samples at 50 – 150-micron thicknesses tended to have breakage and other issues when 90 and 180 degree tests were attempted, a series of tests using tapes and films was devised for comparing their adhesion strength on variously treated glass surfaces. The tapes and films were chosen based on applicability on glass and to cover a range of adhesive strengths. Films used were purchased from www.GrafixArts.com, including a PVC Film with no discernable adhesive layer, commonly used for window decals and adhered by static cling, and Frisket Polypropylene film with an “ultra-low-tack” acrylic adhesive layer which is designed to leave no residue and used for masking and stenciling on glass. The tapes used were both made by 3M Corporation, the Blue tape used was 3M product 8991 which is a polyester tape with silicone non-residue adhesive useful for protection of glass screens during shipping and storage, and the red tape was 3M 850, a polyester tape with a strong acrylic adhesive good for joining, sealing, and packaging applications.

B. Experimental Procedures:

1. Sample Preparation –

Freshly redrawn glass samples were made as previously described and tested immediately on removal from the process to measure contact angle with the Krüss handheld unit and calculate Surface Free Energy. Pellicle samples were also made in the same timeframe to be comparable when estimating SFE by the Wedge test. Samples used for Peel tests were produced by preparing 1” X 6” strips of film and tape ahead of time, and applying them to a sheet of fresh sample, which took a number of seconds longer than the other methods, followed by rolling with a 4-lb rubber wheel to ensure good contact. 1.5” wide samples could then be harvested at leisure (after a 20-hour window of “repose time”) from around the film- and tape-covered areas and secured on steel mounting plates using a high strength double-sided tape (McMaster-Carr Item #77195A2, Polypropylene Cloth with Rubber Adhesive, 90 oz./in. width Adhesion to Steel).

2. Contact angle –

CA measurement was performed by placing the Krüss handheld on the glass and ejecting 0.2-1.0 μ L microdroplets of ultrapure water and diiodomethane onto the glass surface beneath the instrument. Images of the droplets were captured 1-2 seconds after ejection and the angle was either measured automatically with the Krüss-provided software or manually by the operator in more difficult cases. Multiple droplet measurements were made per sample to reduce interpretive error from manual angle assignments, with standard deviations ranging from 1 to 10mN/m. The software used this data and the OWRK method to calculate Surface Free Energy and standard deviation for each sample.

3. T-Peel Tests –

Pellicles were used for the Wedge test as described earlier, as well as various attempts at T-Peel tests. T-Peel was performed by adhering strong tape to both exposed surfaces on one end of a 1” wide strip harvested from a pellicle by scoring both faces and snapping. One piece of tape was clamped in the load cell and the other was adhered to the mounting plate, and the glass strip was supported on the same plane by a piece of Teflon to minimize effects of drag. At low speeds of 3 or 6”/min, the moving platen was driven away from the stationary load cell and the resistive force is measured in grams per inch, relating the average force required to separate a 1” wide sample of the materials at a constant linear speed. This is readily converted into Newtons per meter by a conversion factor of ~0.386 from equation (4)

$$\frac{1 \text{ gram-force}}{1 \text{ inch}} = \frac{0.0098 \text{ N}}{0.0254 \text{ m}} \quad (4)$$

or by using a handy conversion tool for the adhesives industry which can be readily found online²⁶. Since even ultra-thin glass has limited flexibility compared to plastic tape, there was a thickness-dependent bending resistance confounding the ≥ 50 -micron T-peel results to some degree, but 35-micron samples were in line with expected results.

4. 90° and 180° Peel Tests –

90° Peel tests were performed by adhering the harvested film or tape-covered glass sample to a 3” x 12” steel plate which was mounted in a holder set at a 45° angle to the pulling direction, and the clamp on the load cell was set perpendicular to the mounting plate so as the plate moved away, a constant 90° peel angle was maintained (Fig. 8).

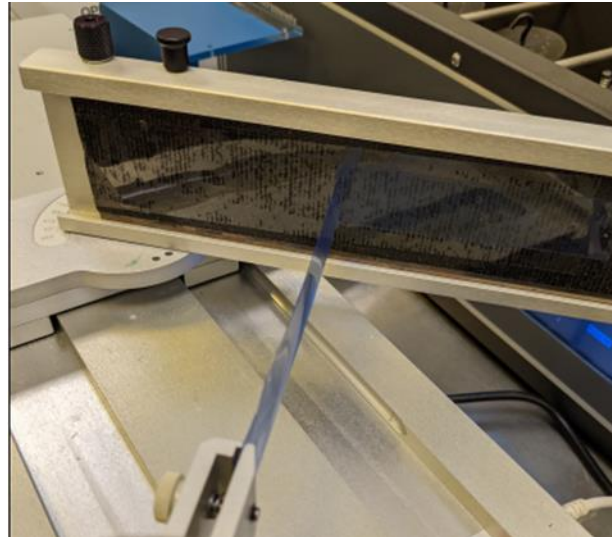


Figure 8 - 90° Peel Test with Blue Tape

The 180° Peel test was done similarly, but the steel mounting plate was held directly on top of the moving plate and the clamp was repositioned to be slightly above the plane of the sample to pull the tape or film without dragging across the sample surface to avoid friction effects. Peel conditions such as speed and travel time were set using on-board controls, as well as time-delay on data collection, to omit unstable results on start-up due to elastic/plastic deformation. Speeds of 3, 6, and 12 in./min were chosen as a variable, with 6 seconds of total travel time for each, and the first one second of data was ignored.

Samples for surface treatments were taken from glass sheets which had been in storage for at least 1 year in cardboard boxes with polymer foam interleaf, held under ambient laboratory conditions. Strips approximately 1.5” x 6” were cut from sheets by scribing and snapping, and subsequently put through the various cleaning treatments,

covered with film or tape, mounted on steel plates with double-stick tape, rolled with a 4-lb wheel, and allowed to rest for 20 hours in the same way as fresh samples.

5. Surface Treatments –

Cleaning treatments were chosen from various relevant options used within Corning Incorporated and throughout glass industry, and based on process availability and minimal complexity to avoid chemically or thermally altering the bulk glass, and is not meant to be an exhaustive list:

- DI Water Rinse, 50°C Dry – Gentle rinse in flowing De-Ionized Water for 1 minute per sample, then placed in clean 50°C oven to dry for >30 minutes.
- DI Water Rinse, 150°C Dry – Gentle rinse in flowing De-Ionized Water for 1 minute per sample, then placed in clean 150°C oven to dry for >30 minutes.
- DI Water Rinse, 450°C Dry – Gentle rinse in flowing De-Ionized Water for 1 minute per sample, then placed in clean 450°C oven to dry for >30 minutes.
- Det. Soak, DI Rinse, 50°C Dry – 30-minute soak in 2% Micro90 Detergent solution at 50°C, gentle rinse in flowing De-Ionized Water for 1 minute per sample, then placed in clean 50°C oven to dry for >30 minutes.
- Acetone Bath / Alcohol Soak / Rinse – Soaked in ultrasonic acetone bath for 10 minutes, followed by three rinses with isopropanol and dried in 50°C oven >30 minutes
- DI Water Rinse / Alcohol Soak / Rinse / 150°C Dry – Gentle rinse in flowing De-Ionized Water for 1 minute per sample, soaked in ultrasonic acetone bath for 10 minutes, followed by three rinses with isopropanol and dried in clean 150°C oven >30 minutes
- Atmospheric Plasma - Gentle rinse in flowing De-Ionized Water for 1 minute per sample, then placed in a Harrick Plasma Model PDC-32G Plasma Cleaner, evacuated and just enough air leaked in to ignite plasma, cleaned 10 minutes.
- Corona Discharge Plasma - Gentle rinse in flowing De-Ionized Water for 1 minute per sample, dried at 50°C, then placed in Enercon ML0182-901-01 Corona-Discharge Plasma Cleaner, cleaned 4 passes at 5 feet/minute with 1000 Watts and watt density of 133 W/ft²/min per pass.

In each case, film or tape was applied at the earliest possible moment (which varied somewhat between treatments from approximately 10 to 30 seconds) and tested approximately 20 hours later to allow “repose time” for the adhesive to settle. Also, attempts were made to form Direct-bonded pellicle samples immediately (again, as soon as possible) after each treatment, but *none were successful*. The Corona-Discharge Plasma came closest to enabling some form of adhesive-less bond between two glass samples which had been plasma-cleaned for multiple consecutive passes and were then able to stick together briefly. However, since they fell apart under their own weight a few seconds later and lacked any evidence of surfaces being actively drawn together the way pellicles do, we believed this to be entirely due to static charge imparted by the plasma which quickly dissipated under ambient conditions.

III. RESULTS AND DISCUSSION

1. SFE by Contact Angle –

Raw	SFE (mN/m)	St. Dv. (mN/m)		IOX	SFE (mN/m)	St. Dv. (mN/m)
Atm Plasma	77.76	1.54		Atm Plasma	77.41	1.73
Fresh	76.50	0.70		Fresh		
DI, 450C	75.74	1.60		DI, 450C	75.74	1.75
Det., 50C	74.19	1.31		Det., 50C	75.73	2.60
Aged >1yr	71.06	2.80		Aged >1yr	63.82	1.68
DI, 150C	70.77	3.57		DI, 150C	63.92	3.91
Alc, 50C	70.13	2.18		Alc, 50C	65.55	3.62
DI, 50C	68.69	4.91		DI, 50C	68.13	4.70
DI, Alc, 150C	45.49	7.49		DI, Alc, 150C	TBD	TBD
C-D Plasma	75.69	1.07		C-D Plasma	TBD	TBD

Table I – Surface Free Energies of Various Glass Samples, calculated via Contact Angle measurements using OWRK method ($\text{mN/m} = \text{mJ/m}^2$)

Normally, when measuring liquid droplet contact angles, surface roughness and droplet size should be accounted for by using the Wenzel equation for “real” surfaces²⁷, as SFE will appear higher due to increased surface under the droplet and errors in actual angle of the surface at the triple phase point compared to the macroscale average surface.

Samples with open porosity may also wick liquid into the pores, skewing the results, and require correction using the Washburn equation²⁸. In our case, all samples were considered “ideal” for this type of measurement as they were non-porous, highly smooth, and relatively clean.

A minimum of three sets of data were used for each natural sample to measure Contact Angle and calculate SFE, and ranked high to low, then compared to ion-exchanged versions which had been treated in the same way. Most results were very similar, but some ion-exchanged samples were lower, probably due to having been contaminated by handling much more than the non-exchanged glass.

2. SFE by Wedge Test –

Glass Modulus	Glass Thickness	Razor Thickness	Crack Length	Critical Strain Energy Release Rate ~ Bonding Energy	Surface Energy = 1/2 Bonding Energy for Identical Surfaces	Converted to gram-force/in.	Predicted T-Peel Strength = 2X SFE
E (Gpa)	t (μm)	y (μm)	L (μm)	$G_c \sim W$ (J/m ²)	γ (mN/m)	(gf/in)	(g/in)
71.5	150	90	5600	0.373	186.33	0.4825965	0.96519
71.5	150	90	5700	0.347	173.59	0.449611	0.89922
71.5	150	90	5800	0.324	161.93	0.4193961	0.83879
71.5	120	90	4600	0.419	209.54	0.5427189	1.08544
71.5	120	90	4700	0.385	192.27	0.4979834	0.99597
71.5	120	90	4800	0.353	176.74	0.4577637	0.91553
71.5	35	90	1780	0.464	231.89	0.6006018	1.2012
71.5	35	90	1880	0.373	186.35	0.4826533	0.96531
71.5	35	90	1840	0.406	203.09	0.5260117	1.05202

Table II - Surface Free Energies of Pellicle Samples via Wedge Test

We found that it was not practical to capture the SFE of freshly redrawn samples by the CA method because even the small amount of time needed to conduct the droplet test on-site already suffered from contamination under ambient lab conditions. The Wedge Test was used to assess these samples at three different sample thicknesses, as shown in Table (2) by the previously described method. These tests turned out to be quite repeatable in all cases predicting near 1g/in Peel Strength.

3. Pellicle T-Peel –

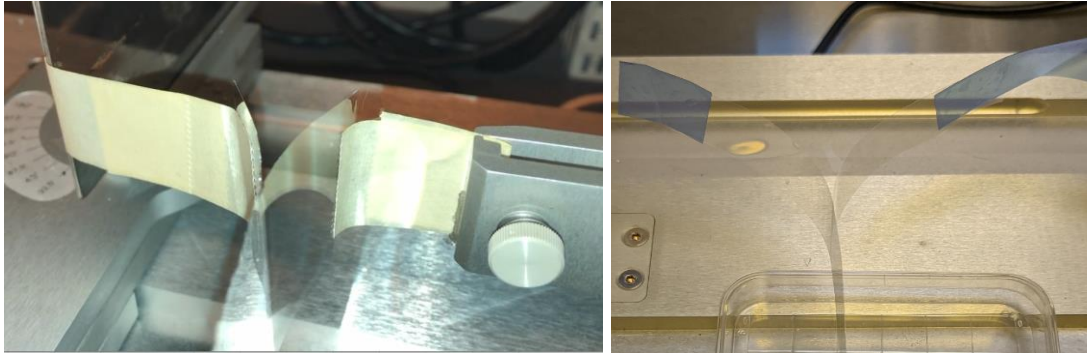


Figure 9 - T-Peel of Pellicles, 50um (Left) and 35um (Right)

Figure 9 shows examples of the T-Peel test as performed on 50 micron and 35 micron thickness pellicle samples by splitting a sample and attaching tabs of strong tape to each piece, then gripping the tabs in the peel tester and pulling them apart at 3 or 6"/min. The T-Peel test is only applicable on very flexible materials, and it seemed that thicknesses of 50 micron and up were too stiff to work properly and read artificially high due to the resistance to bending. 35-micron samples, however, were extremely bendable and closely agreed with the Peel Strength predicted by the wedge test.

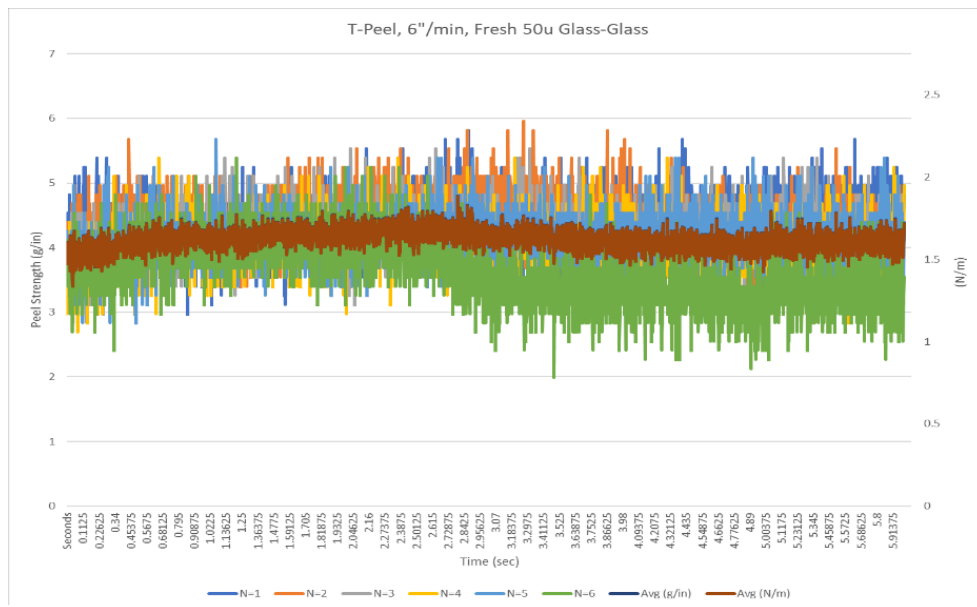


Figure 10 - Measured T-Peel Strength with 50-micron Pellicles

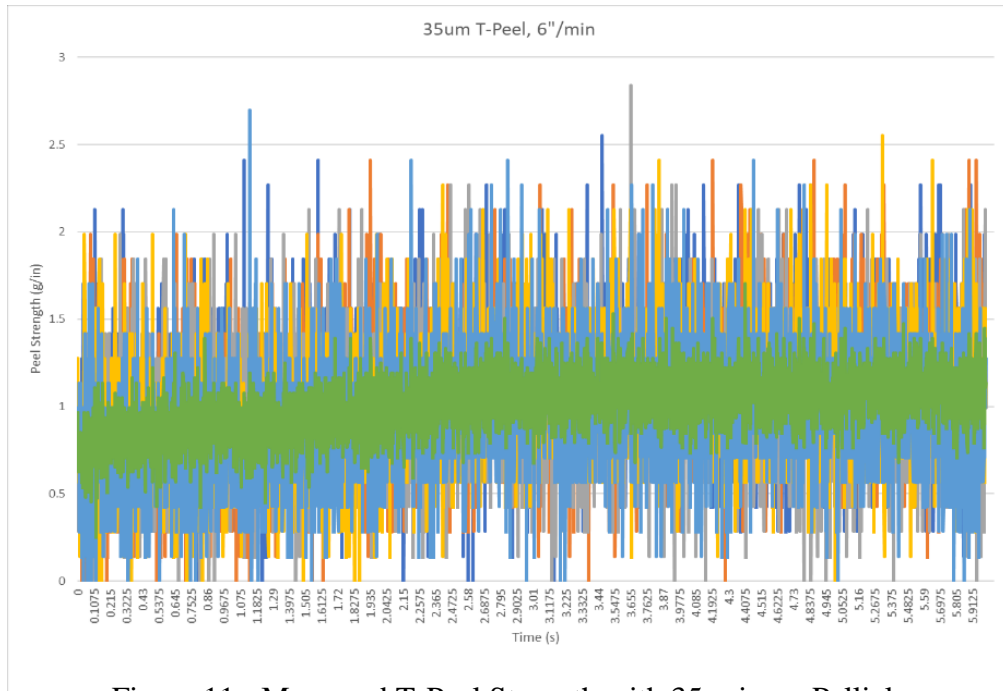


Figure 11 - Measured T-Peel Strength with 35-micron Pellicles

It was known from literature that the glass-glass direct bond can be on the order of the material’s own cohesive strength, yet the pellicle samples peeled apart with very little force. To study this, a set of pellicle samples were made by attaching tabs with increasingly strong adhesives to opposite sides at the very end of the sample, but without initiating separation as was done with previous samples. T-peel tests were run on these samples and in each case, the tabs peeled from the glass without the glasses peeling apart at all. However, when a small crack was made at the edge, the samples fell apart immediately. This is quite similar to how Si wafers at thickness below 100 microns are attached to thicker substrates and withstand mechanical finishing processes, but then are easily separated when heat or a blade is applied to the edge.

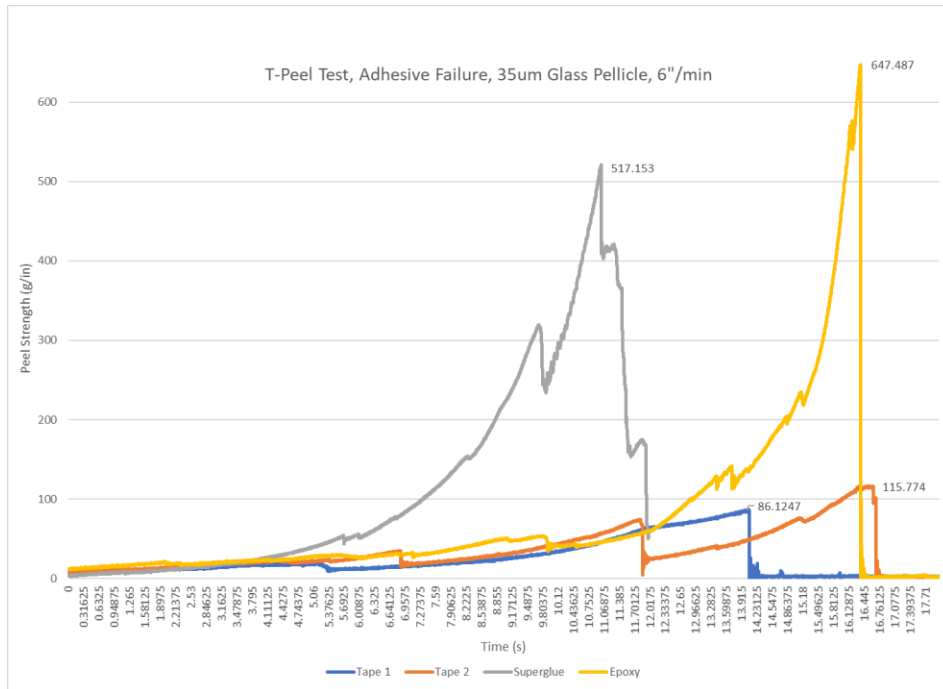


Figure 102 - Adhesive Failure Points Without Pre-Crack

4. Film / Tape Tests –

Given the practical difficulty of handling glass at thicknesses below 50 microns, 100-micron glass samples were used as a surrogate for film and tape peel tests. Three or more “good” measurements were taken at each condition, averaged, and plotted together for comparison. A significant number of measurements were discarded due to breaks in the glass, visible imperfections such as trapped bubbles, or particularly large spreads in the data. A typical dataset is plotted in Fig. 13

100 micron Fresh Glass, 90° Peel, 12"/min



Figure 13 - Peel Strengths of Various Tapes / Films on Fresh Samples

It is readily seen that peel strength increases over two orders of magnitude with various adhesives under identical conditions, and the absolute spread also increases. While this is somewhat expected, the increased variability was not consistent in all cases, and could be impacted by any number of things, including the overall surface quality, effectiveness of treatments, contamination from handling samples, and timing between treatment and application of tape. The issue of assessing data quality independent of scaling proportions will be addressed a little later.

Peel speed is another important factor which effects the measured adhesive strength, and convenient speeds of 3, 6, and 12” per minute were used for these studies, although faster speeds could be perfectly reasonable in certain applications.

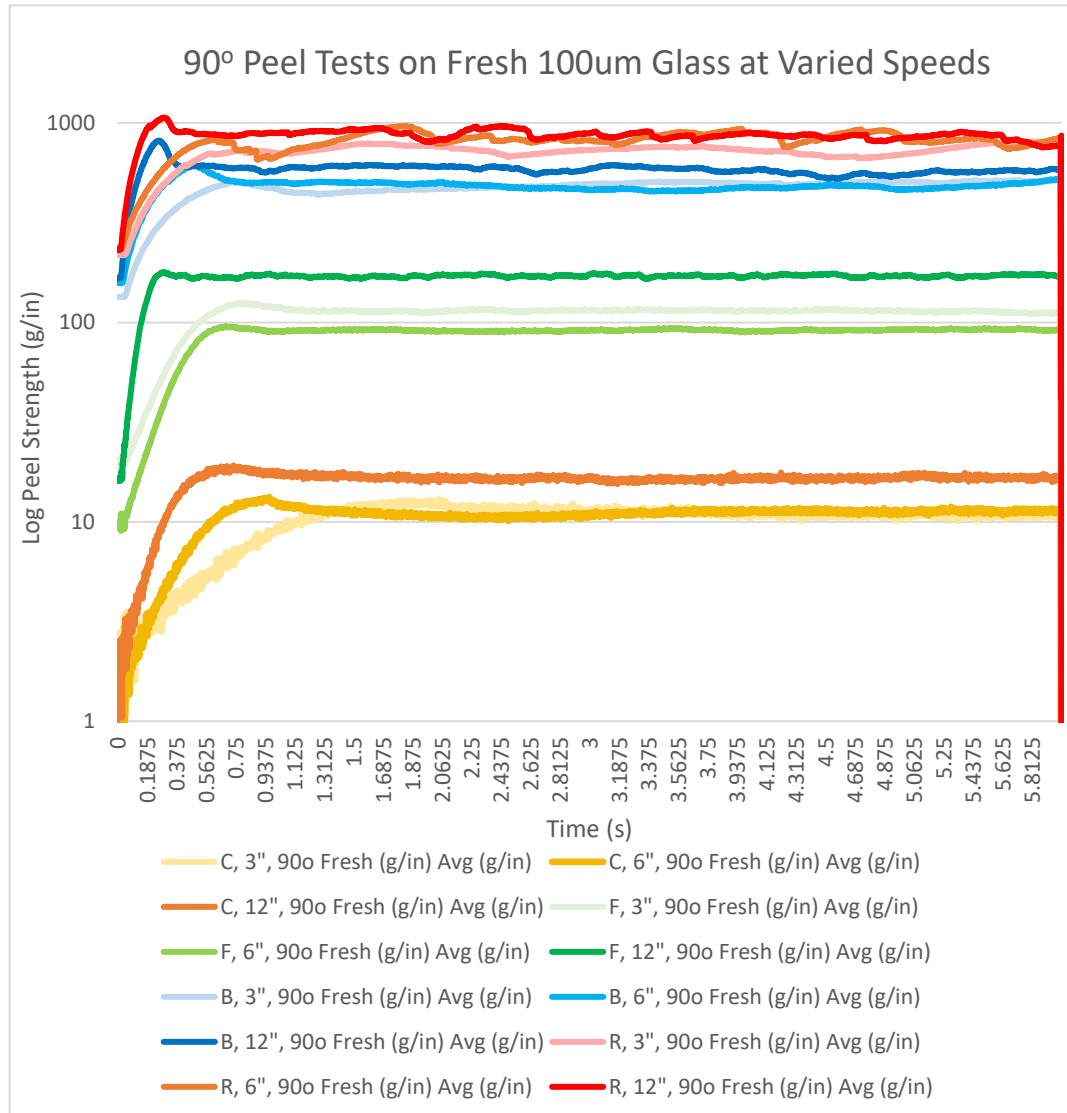


Figure 14 - Peel Strength of Four Tapes on Sister Samples at Various Speeds

As shown in Fig. 14, results from slower speeds closely overlapped, while the highest speed of 12”/min gave noticeably greater values. This subject is discussed by Abbott²⁹, Lacombe³⁰, and others as being due to “viscoelastic effects” involving plastic and elastic deformation of the tape or film as it is being pulled, as well as stretching and “stringing” of the adhesive layer.

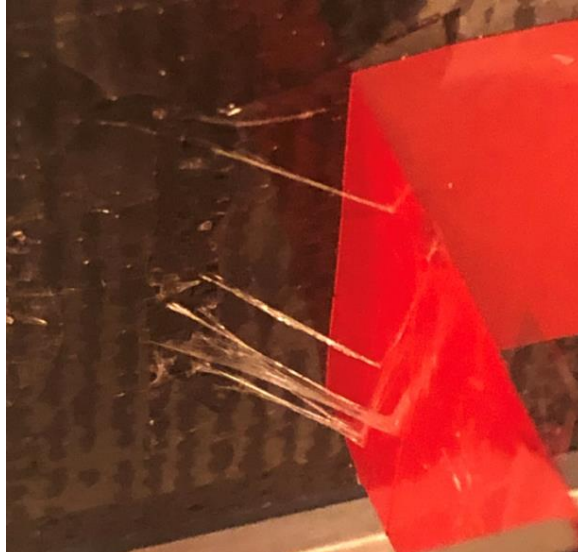


Figure 15 - Adhesive Stringing from Red Tape

The term “Stringing” here refers to the phenomenon where the adhesive stays attached to both surfaces as they separate, forming strings of glue which stretch until they detach or break. Both effects serve to absorb a huge amount of energy and account for a much higher Work of Adhesion than might be expected in many cases. For consistency, this study excluded tests where stringing was observed, which was generally only seen during the initial test of a sample.

At relatively higher speeds or low temperatures, even viscous adhesives may behave in a glassy mode, and can break in a brittle manner by hampering the material’s ability to flow. This can be readily observed by quickly ripping tape from a surface - one will hear a loud staccato sound and see broken patches of adhesive remaining on either surface when compared to slowly peeling the same tape from the same surface. This effect was occasionally seen in our experiments when using red tape at 12”/min, and any such results were also discarded.

5. Film / Tape Tests –

As mentioned previously, many measurements were discarded due to obvious issues, while a few were considered acceptable, but still ranged rather widely. Standard

deviation, which ranged from less than 1 to over 100, was not useful without context, as the peel strengths for different tapes covered three orders of magnitude. To separate the conditional variation from mere proportional rise in standard deviation, this was normalized as the “Coefficient of Variance” (CoV), equal to the Standard Deviation divided by the mean of each data set, after it was trimmed to exclude plastic and elastic deformation effects seen during the first 1.5 seconds of the peel tests.

	SFE (mN/m)	C, 3", 90° (g/in, CoV)	C, 6", 90° (g/in, CoV)	C, 12", 90° (g/in, CoV)	C, 3", 180° (g/in, CoV)	C, 6", 180° (g/in, CoV)	C, 12", 180° (g/in, CoV)
Atm Plas	77.76	13.9, .030	17.3, .015	19.8, .059	13.8, .047	16.9, .041	15.3, .022
Fresh	76.5	14.0, .041	16.4, .032	19.6, .016	9.9, .070	12.6, .035	14.8, .029
DI, 450C	75.74	12.9, .018	15.5, .011	19.2, .018	9.5, .021	12.1, .017	14.4, .018
Det., 50C	74.19	12.8, .034	15.5, .016	18.9, .024	9.4, .074	11.7, .028	13.7, .044
Aged, Raw	71.06	12.6, .023	15.0, .021	18.6, .020	7.7, .025	10.5, .045	12.7, .052
DI, 150C	70.77	12.4, .027	14.8, .017	18.3, .022	7.4, .071	10.5, .056	12.6, .048
Alc, 50C	70.13	12.5, .014	14.3, .015	18.3, .022	7.4, .066	9.7, .031	12.1, .031
DI, 50C	68.69	11.3, .022	14.1, .022	17.8, .017	6.0, .063	9.6, .039	10.5, .034
DI, Alc, 150C	45.49	11.2, .048	12.2, .033	16.9, .027	5.9, .050	7.4, .057	9.0, .052
C-D Plas	75.69	10.1, .028	11.1, .029	16.5, .019	4.6, .110	7.3, .061	8.3, .104

Table III - Average Peel Strengths of Cling Film at Various Conditions

	SFE (mN/m)	R, 3", 90° (g/in, CoV)	R, 6", 90° (g/in, CoV)	R, 12", 90° (g/in, CoV)	R, 3", 180° (g/in, CoV)	R, 6", 180° (g/in, CoV)	R, 12", 180° (g/in, CoV)
Atm Plas	77.76	738.4, .051	847.1, .060	875.4, .049	819.1, .014	865.7, .017	1017, .029
Fresh	76.5	735.6, .020	804.4, .038	866.8, .048	736.6, .006	859.1, .007	964.0, .010
DI, 450C	75.74	666.9, .060	755.9, .012	767.7, .131	703.8, .007	849.5, .015	963.9, .026
Det., 50C	74.19	653.6, .047	731.7, .031	761.8, .056	693.5, .010	793.1, .032	951.8, .023
Aged, Raw	71.06	568.2, .011	650.4, .014	749.8, .035	641.7, .016	736.7, .005	879.7, .004
DI, 150C	70.77	558.4, .018	607.5, .011	718.7, .018	588.9, .005	719.7, .014	865.6, .028
Alc, 50C	70.13	537.5, .018	569.7, .067	716.6, .078	528.4, .028	648.4, .017	829.1, .053
DI, 50C	68.69	449.3, .042	565.0, .034	613.4, .024	524.0, .026	599.7, .016	767.4, .030
DI, Alc, 150C	45.49	436.7, .030	487.5, .025	600.5, .041	498.7, .007	593.8, .032	730.6, .029
C-D Plas	75.69		486.6, .024	592.3, .031	495.7, .027	575.4, .023	657.2, .050

Table IV - Average Peel Strengths of Frisket Film at Various Conditions

	SFE (mN/m)	F, 3", 90° (g/in, CoV)	F, 6", 90° (g/in, CoV)	F, 12", 90° (g/in, CoV)	F, 3", 180° (g/in, CoV)	F, 6", 180° (g/in, CoV)	F, 12", 180° (g/in, CoV)
Atm Plas	77.76	114.2, .011	131.3, .015	171.2, .012	131.6, .045	146.2, .011	429.4, .021
Fresh	76.5	108.2, .017	130.5, .011	159.7, .013	120.8, .011	137.0, .040	192.7, .025
DI, 450C	75.74	107.6, .009	130.0, .023	158.5, .030	102.8, .012	133.8, .014	180.6, .055
Det., 50C	74.19	103.4, .018	118.7, .012	147.9, .013	93.7, .022	129.4, .010	179.5, .011
Aged, Raw	71.06	97.5, .010	116.0, .013	146.8, .016	90.9, .014	113.0, .050	155.8, .021
DI, 150C	70.77	94.6, .014	113.6, .018	144.8, .011	76.0, .010	102.3, .012	139.7, .016
Alc, 50C	70.13	85.9, .037	103.7, .018	135.1, .013	75.0, .012	100.2, .008	137.5, .047
DI, 50C	68.69	84.9, .016	100.0, .020	114.6, .143	74.5, .019	92.0, .030	134.3, .017
DI, Alc, 150C	45.49	65.7, .018	91.4, .009	108.2, .029	69.5, .020	91.9, .011	126.7, .019
C-D Plas	75.69	63.7, .013	82.0, .033	81.5, .103	55.5, .012	90.0, .024	108.8, .031

Table V - Average Peel Strengths of Blue Tape at Various Conditions

	SFE (mN/m)	B, 3", 90° (g/in, CoV)	B, 6", 90° (g/in, CoV)	B, 12", 90° (g/in, CoV)	B, 3", 180° (g/in, CoV)	B, 6", 180° (g/in, CoV)	B, 12", 180° (g/in, CoV)
Atm Plas	77.76	630.6, .007	641.3, .033	647.6, .023	842.8, .003	855.5, .008	914.0, .006
Fresh	76.5	612.2, .024	623.6, .016	642.7, .015	756.9, .007	812.0, .017	900.8, .019
DI, 450C	75.74	587.2, .005	603.4, .018	622.1, .044	755.5, .019	796.9, .008	891.9, .018
Det., 50C	74.19	570.6, .005	591.1, .007	608.6, .013	754.3, .011	782.6, .046	889.6, .032
Aged, Raw	71.06	565.0, .007	589.8, .017	600.4, .025	726.9, .020	767.2, .019	882.1, .077
DI, 150C	70.77	553.5, .013	585.2, .011	596.0, .072	726.1, .005	765.5, .011	875.6, .010
Alc, 50C	70.13	546.3, .020	558.0, .016	585.2, .066	677.4, .005	751.0, .026	853.6, .028
DI, 50C	68.69	493.8, .011	536.2, .022	580.4, .038	676.2, .010	724.0, .027	850.5, .018
DI, Alc, 150C	45.49	493.7, .034	516.8, .031	580.0, .056	675.2, .011	723.3, .011	842.7, .016
C-D Plas	75.69	432.0, .016	478.9, .031	488.4, .119	548.0, .011	711.9, .017	787.9, .007

Table VI - Average Peel Strengths of Red Tape at Various Conditions

6. Elastic / Plastic Effects –

Lastly, it must be noted that the peel strength as measured by the test instrument is many times larger than what experts in the field might consider “true adhesion”³¹. In brief, this is entirely due to elastic-plastic effects on the tape and adhesive during the peel test. Such deformations are responsible for most of the work expended by the machine and can make the results very misleading.

A simplified elastic model of 90° Peel presented by Lacombe³² states that

$$p (1 - \cos \theta) = \gamma \quad (5)$$

where p is the peel load per unit width of the peel strip and γ is the work required to separate the two surfaces.

For 90° Peel: $(1 - \cos \theta) = (1 - 0) = 1 \quad (6)$

Therefore, $p = \gamma \quad (7)$

In fact, however, almost all cases do exhibit plastic deformation, so actually

$$p = \gamma + \psi \quad (8)$$

where the function ψ represents the energy dissipation rate by the entire system (elastic and plastic deformations) per unit advance of the peel strip.

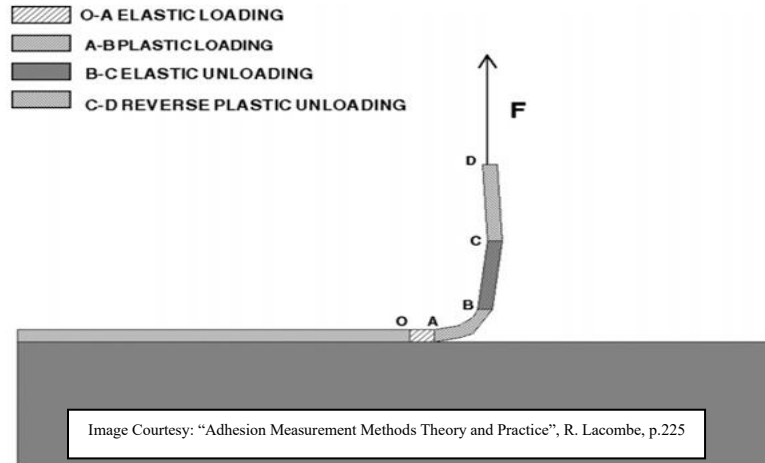


Figure 16 – “Schematic of the bending process” by Lacombe, Applied Adhesion Testing, reprinted with permission via CCC

According to Abbott³³, one may ignore the effects of plastic deformation if the peel strip is above a critical thickness, t_c , which is calculated from known values:

$$t_c = \frac{3EP}{\sigma^2} \quad (9)$$

where E is Young’s Modulus, σ is yield strength, and P is measured peel force. Using these results produces a table of max-min values of critical thicknesses:

Material	t_{actual} (m)	t_c (m)	E (Pa)	Peel (N/m)	σ (Pa)
Cling	1.80E-04	5.89E-06	3.30E+09	1.8	5.50E+07
PVC		2.55E-05	3.30E+09	7.8	5.50E+07
Frisket	5.08E-05	1.90E-04	1.95E+09	22	2.60E+07
Polypropylene		4.41E-04	1.95E+09	51	2.60E+07
Blue Tape	2.60E-05	2.30E-04	4.50E+09	170	1.00E+08
Polyester		4.86E-04	4.50E+09	360	1.00E+08
Red Tape	2.30E-05	2.31E-04	4.50E+09	171	1.00E+08
Polyester		5.27E-04	4.50E+09	390	1.00E+08

Table VII - Max - Min Values of Critical Thickness vs. Actual

The PVC Cling Film is the only one above critical thickness, so it is worth trying to address the plastic deformation in the other three cases by obtaining the energy dissipation function ψ for each system.

This function is rather difficult to calculate from modeling or measured values and somewhat beyond the ability of the equipment used here. Fortunately, it can be estimated by a method suggested by Kim and Kim³⁴ using a “Universal Peel Diagram” where normalized values calculated from the tape properties (thickness, elastic modulus, yield strength) and peel force measurements are plotted on a special scale which they developed. The raw data point is then adjusted such that the scaling relationship, η , from the raw data coincides with η' calculated from known values as shown in the example data on the following graph.

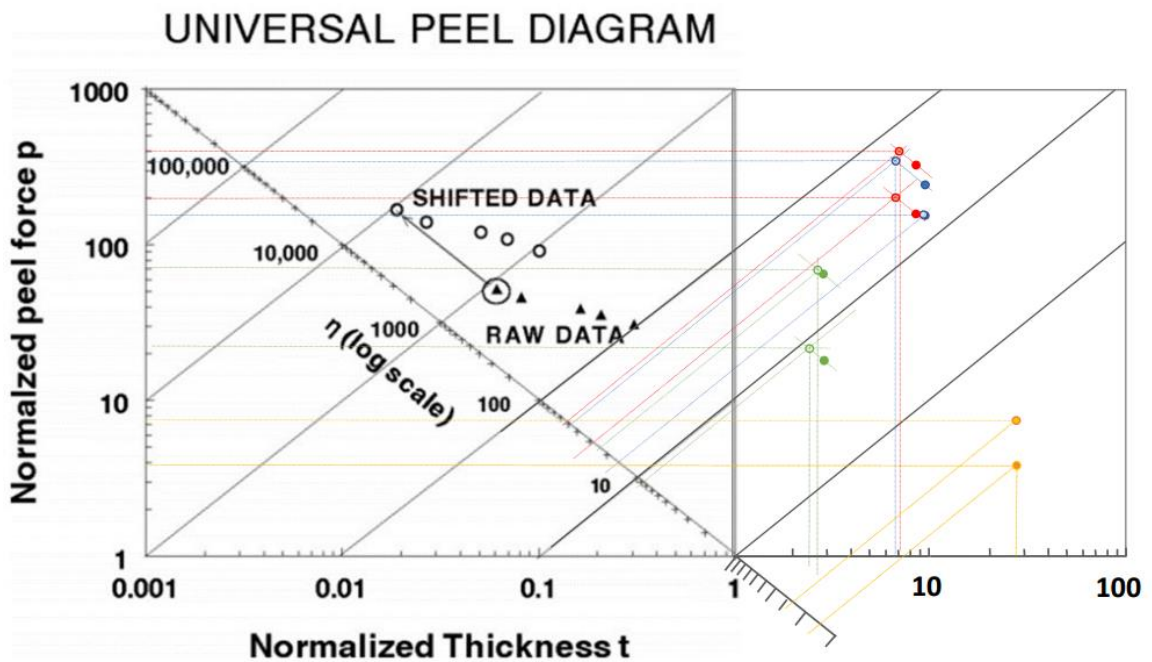


Figure 17 – “Universal Peel Diagram” by Kim, K.-S., Kim J., reprinted with permission via CCC, Extrapolated from Original to Cover Data

This new point yields a new peel force and thickness, p' and t' , which can be substituted into Kim’s formulas to give an “actual” work of separation, γ' , such that the remainder must equal the dissipation function, ψ .

$$\text{a) } \mathbf{p} = \frac{P}{\gamma} \quad (\text{Normalized peel force}) \quad (10.1)$$

$$\text{b) } \mathbf{t} = \frac{\sigma_0^2 t}{6E\gamma} \quad (\text{Normalized film thickness}) \quad (10.2)$$

$$\text{c) } \boldsymbol{\eta} = \frac{6Ep}{\sigma_0^2 t} \quad (\text{Force/thickness ratio}) \quad (10.3)$$

$$\text{d) } \boldsymbol{\eta} = \frac{P}{t} \quad (\text{Scaling relationship}) \quad (10.4)$$

Note that this method was developed for metallic films with little or no elastic deformation, but the trends and comparisons still apply for polymeric peel strips, even if the values are not absolutely correct. These were calculated for present data set as shown:

material	t _{actual} (m)	Y	E (Pa)	p (g/in)	σ (Pa)	p (N/m)	t	η	t'	p'	η'	Y'
Cling	1.80E-04	1	3.30E+09	10.1	5.50E+07	3.9	27.50	0.14	0.15	3.90	26.00	2.59
PVC Film	1.80E-04	1	3.30E+09	19.8	5.50E+07	7.6	27.50	0.28	0.27	7.60	28.15	2.61
"Frisket"	5.08E-05	1	1.95E+09	63.7	2.60E+07	24.6	2.94	8.38	2.40	23.00	9.58	2.77
Polypropylene	5.08E-05	1	1.95E+09	171.2	2.60E+07	66.1	2.94	22.51	2.70	71.00	26.30	2.41
Blue Tape	2.60E-05	1	4.50E+09	432	1.00E+08	166.8	9.63	17.32	9.50	170.00	17.89	2.54
Polyester	2.60E-05	1	4.50E+09	647.6	1.00E+08	250.0	9.63	25.96	6.80	350.00	51.47	1.85
Red Tape	2.30E-05	1	4.50E+09	436.7	1.00E+08	168.6	8.52	19.79	6.80	205.00	30.15	2.13
Polyester	2.30E-05	1	4.50E+09	875.4	1.00E+08	337.9	8.52	39.67	7.05	400.00	56.74	2.19

Table VIII - Normalized Values Extrapolated from Universal Peel Diagram

It is very interesting given the very wide range of input \mathbf{p} that the actual work of adhesion, γ' , which should equal peel strength for a 90° peel test, is consistently about 2-2.5 N/m and is reminiscent of the comparably small range of Surface Free Energies obtained from Contact Angle measurements. This would seem to support the argument that all true adhesion is at similarly low levels and that the seemingly high experimental values stem from energy absorption by deformation of adhesive and adherend materials.

IV. SUMMARY AND CONCLUSIONS

It was hypothesized that freshly redrawn glass samples would show the highest Surface Free Energy and adhesion values due to it consisting primarily of newly created surface in proportion to the redraw ratio and retaining excellent smoothness from the

Fusion production process. With time and exposure to atmosphere, the quality of the surface is bound to degrade due to adsorption of water, CO₂, hydrocarbons, particulate and fibrous debris, and any number of other contaminants which impede the molecular-scale contact which is required for strong direct bonding.

The hypothesis was demonstrated empirically by analyzing freshly made samples as immediately as possible from the time it emerged from the redraw process and then comparing to aged samples from long-term storage. Interestingly, SFE did not reduce in any measurable way over short timescales when calculated from contact angle using the OWRK method and was only slightly lower for multi-year aged samples directly out of storage. This was in stark contrast to the inability to make direct-bonded pellicle samples from any but the freshest glass pieces, even when only aged for a few minutes, suggesting that SFE does not tell the entire story. This is also supportive of the position of Dr. Abbott and many others that the high SFE which accompanies very clean surfaces may be needed to support adhesion initially, either to enhance wettability of an adhesive layer or simply enabling true surface contact at the molecular scale. A perfectly clean, dry, smooth surface lacks contaminant molecules which would physically interfere with “van der Waals” or hydrogen bonding by limiting contact at sub-nanometer (0.2 - 0.5nm) distances and lower SFE by bonding to exposed surface molecules. However, heroic efforts to raise it above a certain value leads to very poor returns when it comes to enhancing PSA adhesion strength.

It can also be seen that the information gathered by various peel tests may not be inherently useful at determining the true adhesion of a system, in that widely ranging values can arise from very similar SFE and Work of Adhesion results. But, with a large enough data set and carefully controlled experiments, such studies can be practical in ranking the general effectiveness of various surface treatments within a given system.

Finally, it was shown that the glass – glass direct bond obtained by immediate formation of pellicle samples with newly created surfaces were both exceptionally weak by normal peel testing with values even less than cling film or sticky notes, but also exceptionally strong prior to crack initiation such that even strong tapes, superglue, and

epoxy peeled from the glass surfaces rather than pull them apart. This explains the usefulness of similar techniques in ultrathin Si-wafer finishing where direct bonding to a stiff substrate withstands vigorous mechanical forces but peels apart without damaging the wafer and leaves no residue.

V. REFERENCES

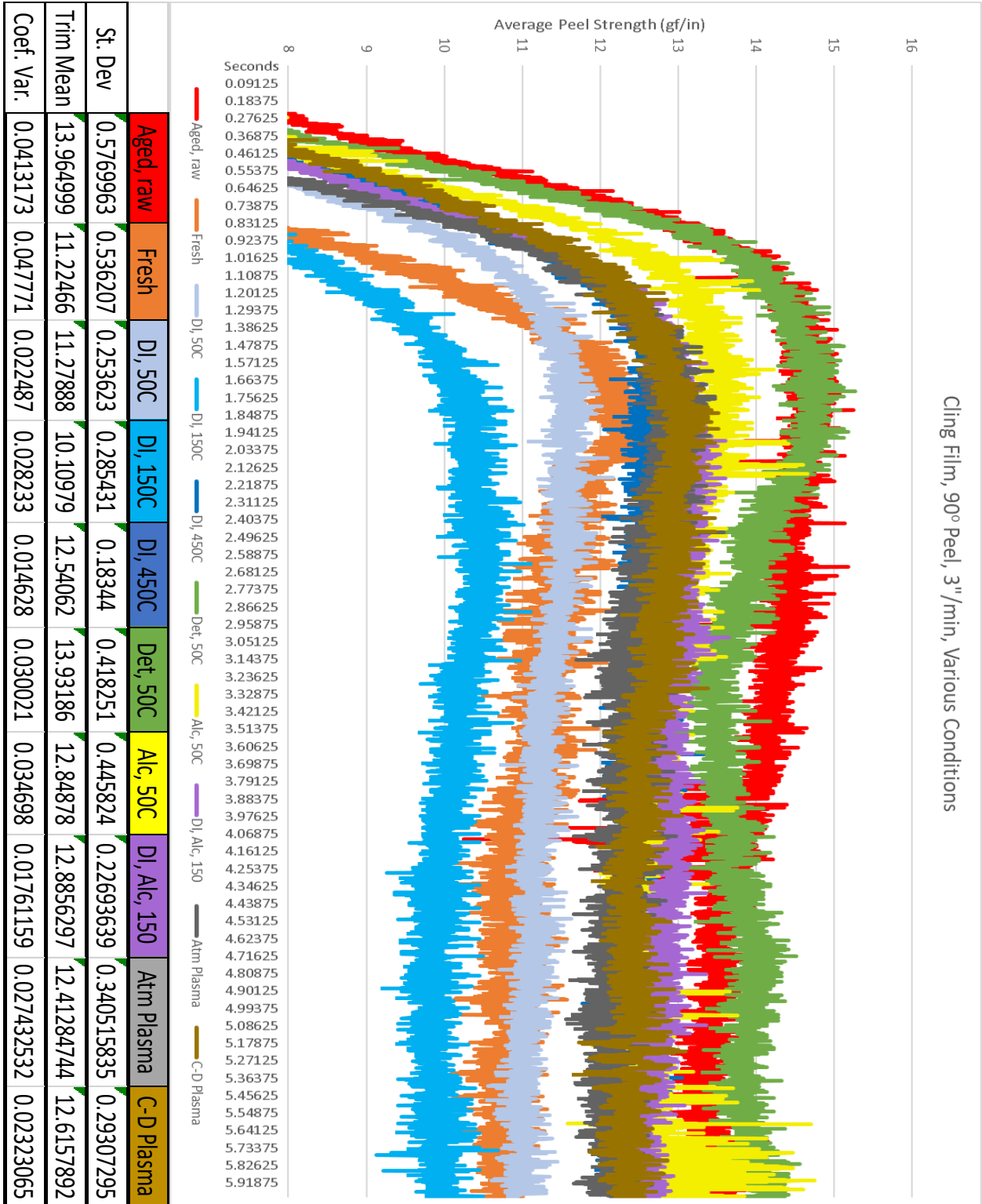
1. *History of Glass Home Page*. <https://historyofglass.com> (Accessed 2021-10-21).
2. *The World of Glass, Applications*.
<https://www.glassallianceeurope.eu/en/applications> (Accessed 2021-10-21).
3. Clark C. C.; Yudenfriend H.; Redner A. S. Laceration and ejection dangers of automotive glass, and the weak standards involved. The strain fracture test. *Annu Proc Assoc Adv Automot Med*. **2000**, *44*, 117-131.
4. Morse, D.L.; Evenson, J. W. Welcome to the Glass Age, *Int'l Journal of Applied Glass Science*. **2016**, *7* (4), 117-132. DOI: 10.1111/ijag.12242
5. Lin, S. B.; Durfee, L. D.; Ekeland, R. A.; McVie, J.; Schalau G. K. Recent advances in silicone pressure-sensitive adhesives. *Journal of Adhesion Science and Technology*. **2007**, *21* (7), 605-623. DOI: 10.1163/156856107781192274
6. Walker, P. J. Organosilanes as adhesion promoters, *Journal of Adhesion Science and Technology*. **1991** *5* (4), 279-305. DOI: 10.1163/156856191X00369
7. Demonstration by Vaz Zastera at Corning Museum of Glass, 8/29/2007, and on *Optical Contacting Page*. http://www.zartwerks.com/optical_contacting.html
8. Myatt, C.; Traggis, N.; Dessau, K. Optical Fabrication: Optical Contacting Grows More Robust. *Laser Focus World*, **2006** *42* (1), 95-98.
9. Kendall, K. *Molecular Adhesion and Its Applications - The Sticky Universe*; Kluwer Academic Publishers, 2004.
10. Abbott, S. *Adhesion Science Principles and Practice*; DEStech Publications Inc., 2015.
11. Scudellari, M. N95 Masks' Efficiency Can Be Restored With Electricity: Smart Masks May Follow. *IEEE Spectrum*, Sep. 14, 2020.
12. Whalen, J. M.; Fekety, C.; Filippov, A.; Osterhout, C. D.; Cheng, S-C.; Truesdale, C. Nanoparticle Synthesis Using a Two-Stage Spray Pyrolysis Generator, Poster #160e, *Particle Technology Forum, AIChE Annual Meeting*, 11/13/2006

13. Agnello, G.; Manley, R.; Smith, N.; LaCourse, W.; Cormack, A. Triboelectric properties of calcium aluminosilicate glass surfaces. *International Journal of Applied Glass Science*. **2017**, *9* (1), 3-15. <http://dx.doi.org/10.1111/ijag.12276>.
14. Elmer, T. H. Porous and Reconstructed Glasses. in *Engineered Materials Handbook*, Vol. 4. *Ceramics and Glasses*, ASM International, 1992; pp 427-432
15. Smay, G. L.; Wasylyk, J. S.; Southwick, R. D. A critical assessment of lubricating and damage-preventive glass coatings. in *The Eitel Institute for Silicate Research, Third Proceeding of the Symposium*, University of Toledo, March 22, 1982, p 39.
16. Beggans, M. H. Ultrathin Silicon Wafer Bonding Physics and Applications. Ph.D. Dissertation, New Jersey Institute of Technology, Newark NJ, 2001. <https://digitalcommons.njit.edu/dissertations/464> (Accessed 2021-10-21).
17. Abbott, S. *Adhesion Science Principles and Practice*; DEStech Publications Inc., 2015, pp. 25-30
18. Private Communication, P. Mazumder, Corning Incorporated
19. <https://www.corning.com/worldwide/en/innovation/the-glass-age/science-of-glass/how-it-works-corning-fusion-process.html> (Accessed 2021-10-21).
20. Cimo, P. J.; Murtagh, M. T.; Powley, M. L. Process and device for manufacturing glass sheet. US 7770414, 2010
21. Peng, J.; Snyder, G. J. A Figure of Merit for Flexibility. *Science*. **2019**, *366* (6466), 690-691. DOI: 10.1126/science.aaz5704
22. Lilienfeld, P. Optical Detection of Particle Contamination on Surfaces: A Review. *Aerosol Science and Technology*, **1986** *5* (2), 145-165
DOI: 10.1080/02786828608959085
23. *Newton's rings*. in *Encyclopedia Britannica*. Britannica.com, 2019, <https://www.britannica.com/science/Newtons-rings> (Accessed 2021-10-21).
24. Kruss Scientific webpage on Owens, Wendt, Rabel and Kaelble (OWRK) method. <https://www.kruss-scientific.com/en-US/know-how/glossary/owens-wendt-rabel-and-kaelble-owrk-method> (Accessed 2021-10-21).
25. Maurel-Pantel A.; Voisin, M.; Bui, Q.; Cocheteau, N.; Lebon, F.; Hochard, C. A cohesive zone model for fracture initiation and propagation of fused silica direct bonding interface. *Engineering Fracture Mechanics* **2019**, *219* (2), 106649. DOI: 10.1016/j.engfracmech.2019.106649
26. www.tenacioustapes.com.au/adhesive-tapes-conversions. (Accessed 9-3-21)

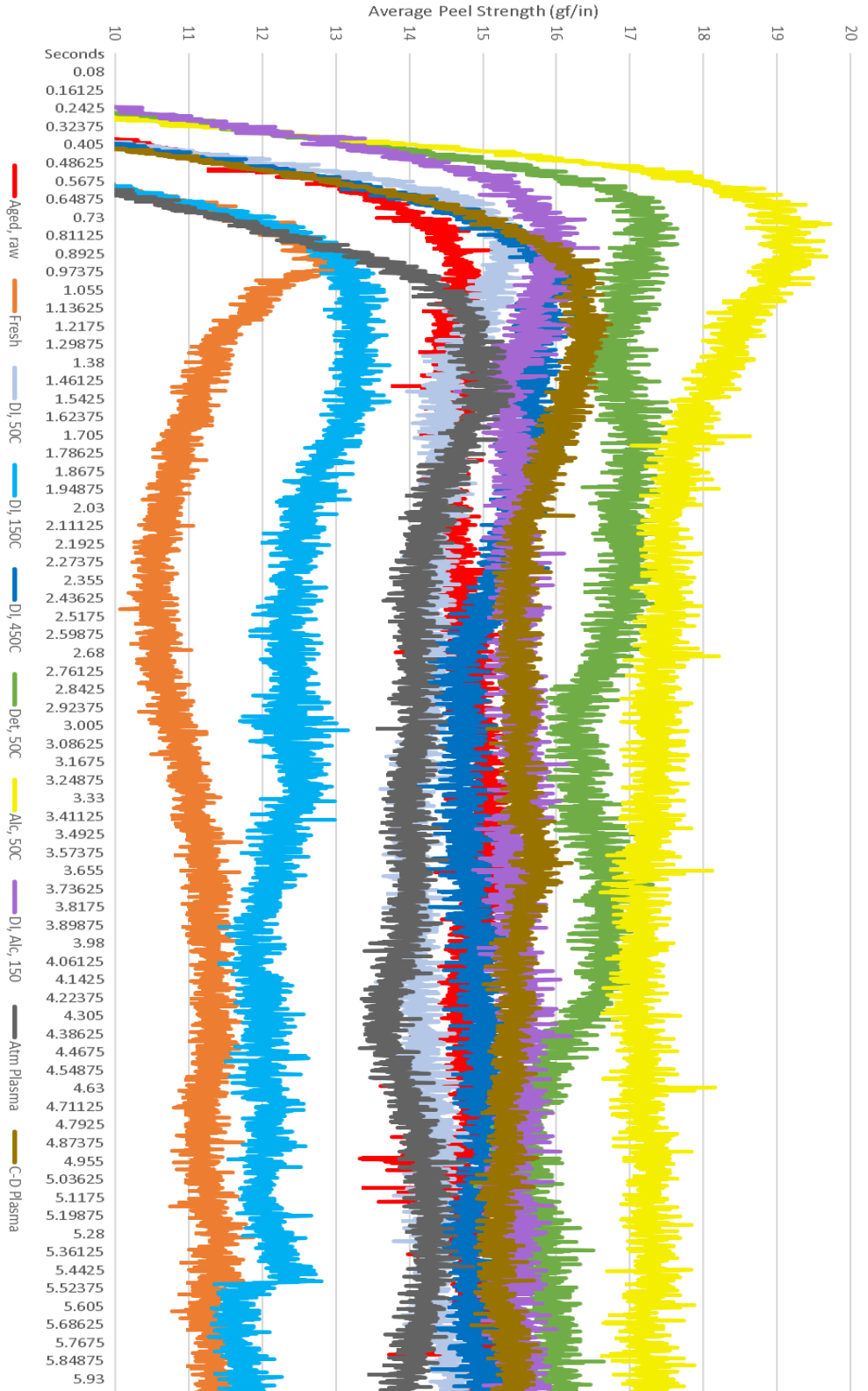
27. Wenzel, R.W. Resistance of solid surfaces to wetting by water. *Industrial & Engineering Chemistry* **1936**, 20, 988
28. Chibowski, E.; Hoyslsz, L. Use of the Washburn Equation for Surface Free Energy Determination. *Langmuir* **1992**, 8, 710-716
29. Abbott, S. *Adhesion Science Principles and Practice*; DEStech Publications Inc., 2015, pp. 201-203
30. Kendall, K. *Molecular Adhesion and Its Applications - The Sticky Universe*; Kluwer Academic Publishers, 2004. p.349
31. Lacombe, R. *Adhesion Measurement Methods, Theory and Practice*, CRC Press Taylor & Francis Group, 2006. pp.196-197
32. Lacombe, R. *Adhesion Measurement Methods, Theory and Practice*; CRC Press Taylor & Francis Group, 2006. pp. 224-231
33. Abbott, S. *Adhesion Science Principles and Practice*; DEStech Publications Inc., 2015, pp. 207-209
34. Kim, K.-S.; Kim J. Elasto-Plastic Analysis of the Peel Test for Thin Film Adhesion. *Journal of Engineering Materials and Technology* **1988**, (110), 266. DOI:10.1115/1.3226047

VI. APPENDIX

Additional Data – Averaged results from Tape / Film Peel Tests (See Tables III – VI)

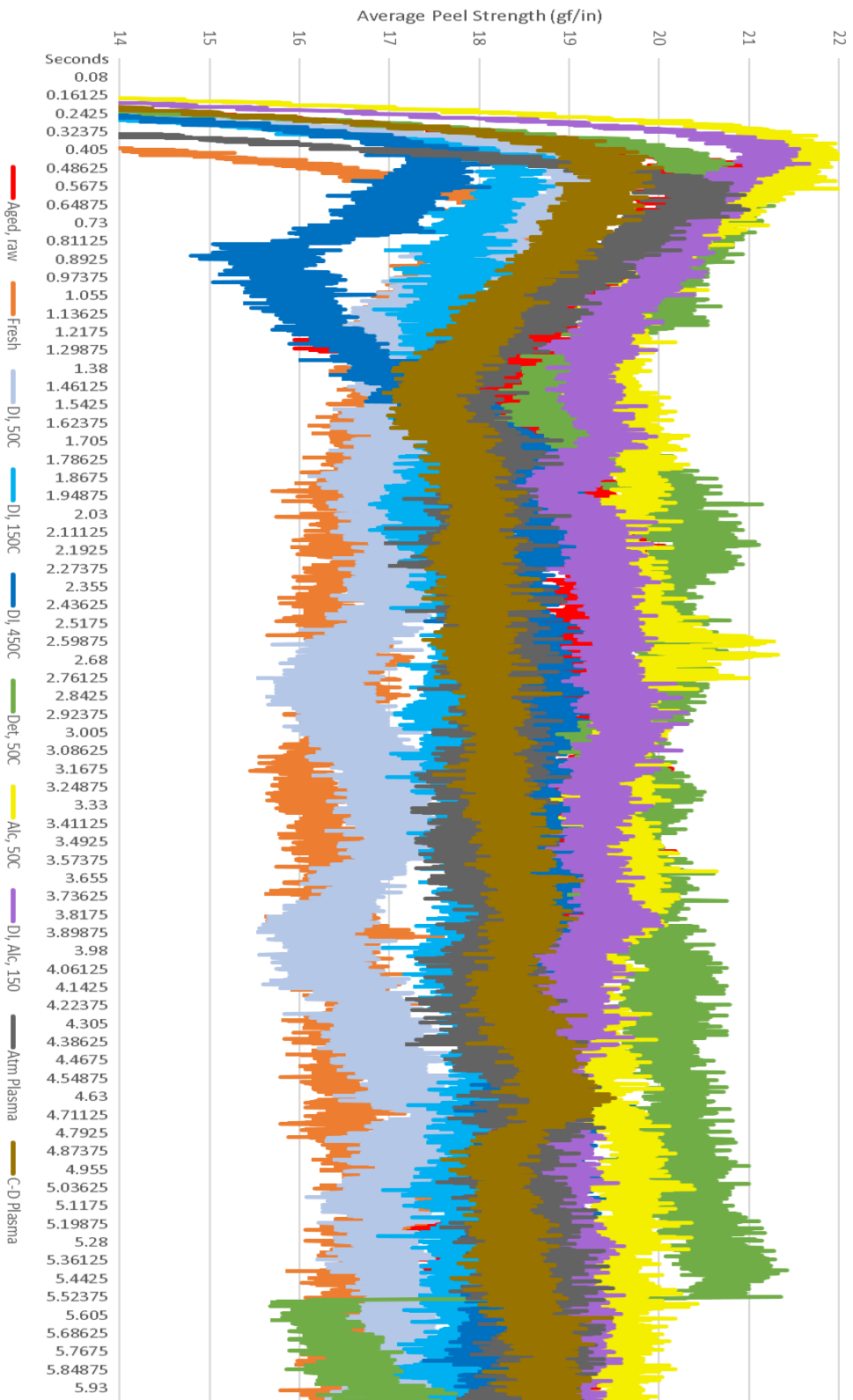


Cling Film, 90° Peel, 6"/min, Various Conditions



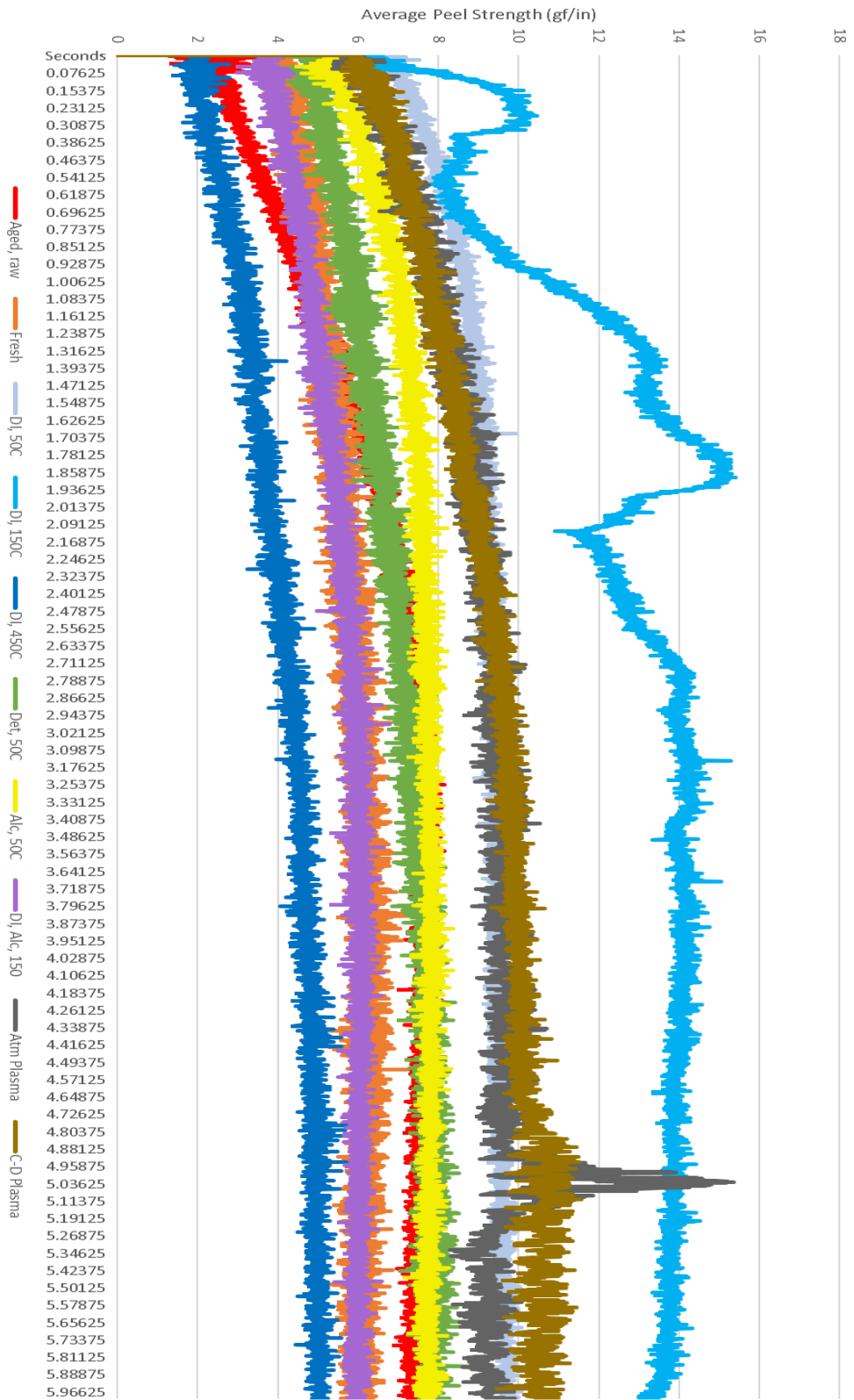
	Aged, raw	Fresh	DJ, 50C	DJ, 150C	DJ, 450C	Det, 50C	Aic, 50C	DJ, Aic, 150	Atm Plasma	C-D Plasma
St. Dev	0.25052237	0.31947633	0.21848365	0.39826716	0.31363082	0.5176748	0.26473504	0.17551559	0.3063442	0.2527746
Trim Mean	14.8241389	11.0709788	14.2595309	12.2226117	14.976749	16.364062	17.3108726	15.4634108	14.1046497	15.474318
Coef. Var.	0.01689962	0.0288571	0.01532194	0.03258446	0.02094118	0.03163486	0.01529299	0.01135038	0.02171938	0.0163351

Cling Film, 90° Peel, 12"/min, Various Conditions



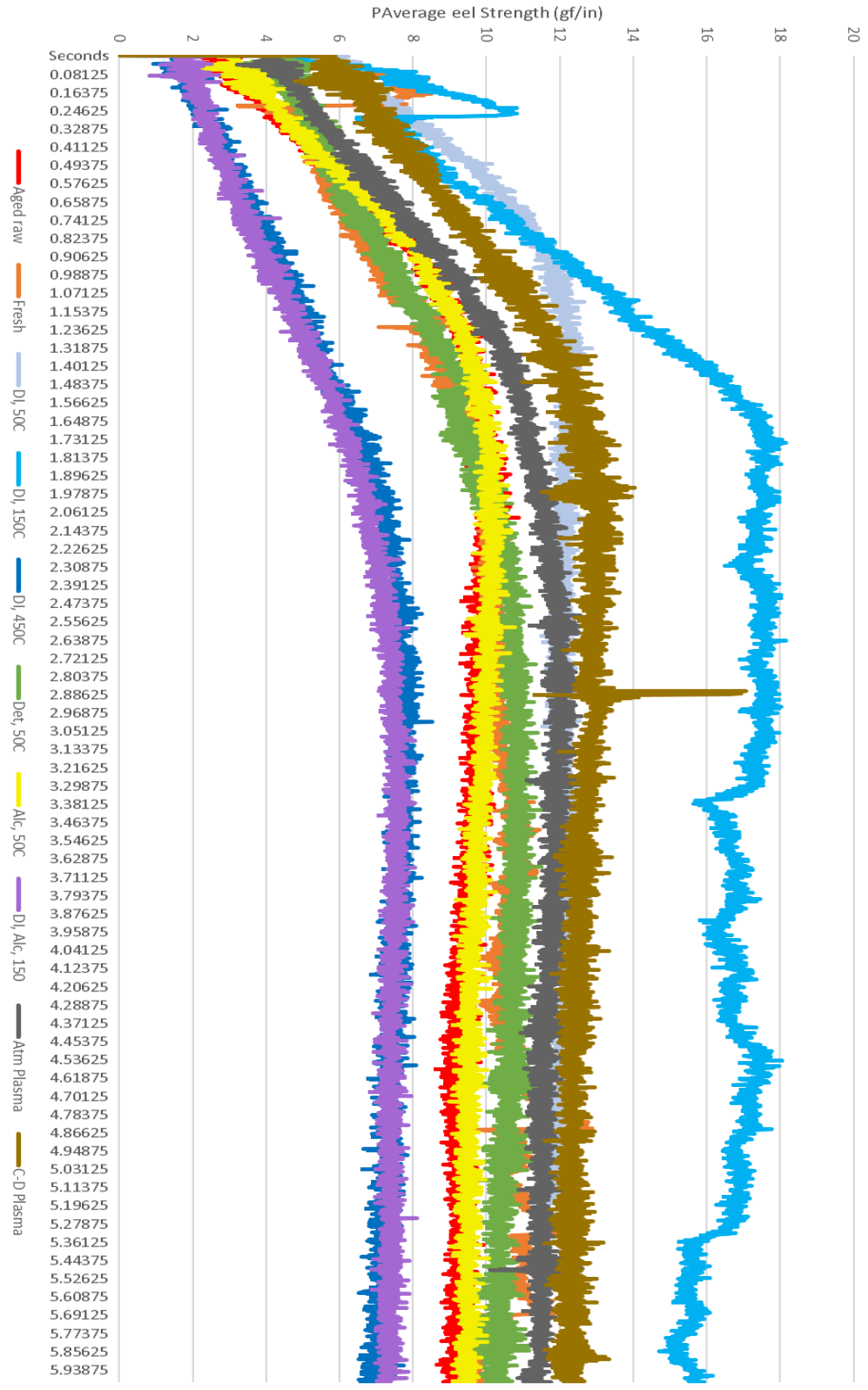
	Aged, raw	Fresh	DI, 50C	DI, 150C	DI, 450C	Det, 50C	Alc, 50C	DI, Alc, 150	Atm Plasma	C-D Plasma
St. Dev	0.45427128	0.31298145	0.45219955	0.296812	0.37301489	1.16096692	0.32257446	0.34774807	0.39878301	0.39765827
Trim Mean	18.9437299	16.5208522	16.8933967	17.7910516	18.5727351	19.7794947	19.6181206	19.1808752	18.2547259	18.2834974
Coef. Var.	0.02398003	0.01894463	0.02676783	0.01668322	0.020084	0.05869548	0.01644268	0.01812994	0.02184547	0.02174957

Cling Film, 180° Peel, 3"/min, Various Conditions



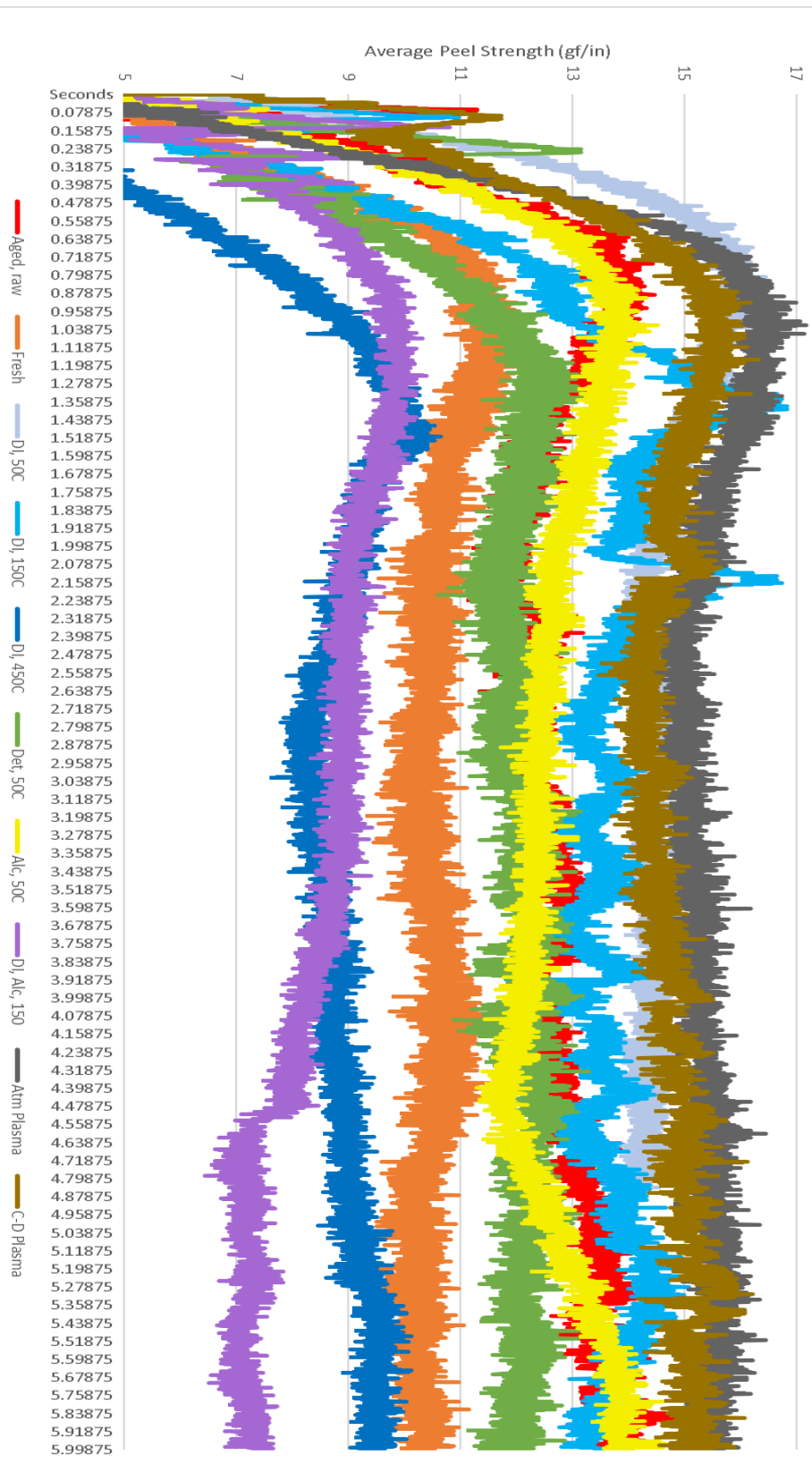
	Aged, raw	Fresh	D1, 50C	D1, 150C	D1, 450C	Det, 50C	Alc, 50C	D1, Alc, 150	Atm Plasma	C-D Plasma
St. Dev	0.48894765	0.37958089	0.19675983	0.64562787	0.50184566	0.53182819	0.19260315	0.29561993	0.69498946	0.69330689
Trim Mean	7.37304161	6.03662462	9.45496754	13.7999475	4.56173393	7.44670025	7.73587043	5.90608742	9.42013081	9.87316556
Coef. Var.	0.0663156	0.06287966	0.02081021	0.04678481	0.11001204	0.07141797	0.02489741	0.05005343	0.07377705	0.07022134

Cling Film, 180° Peel, 6"/min, Various Conditions



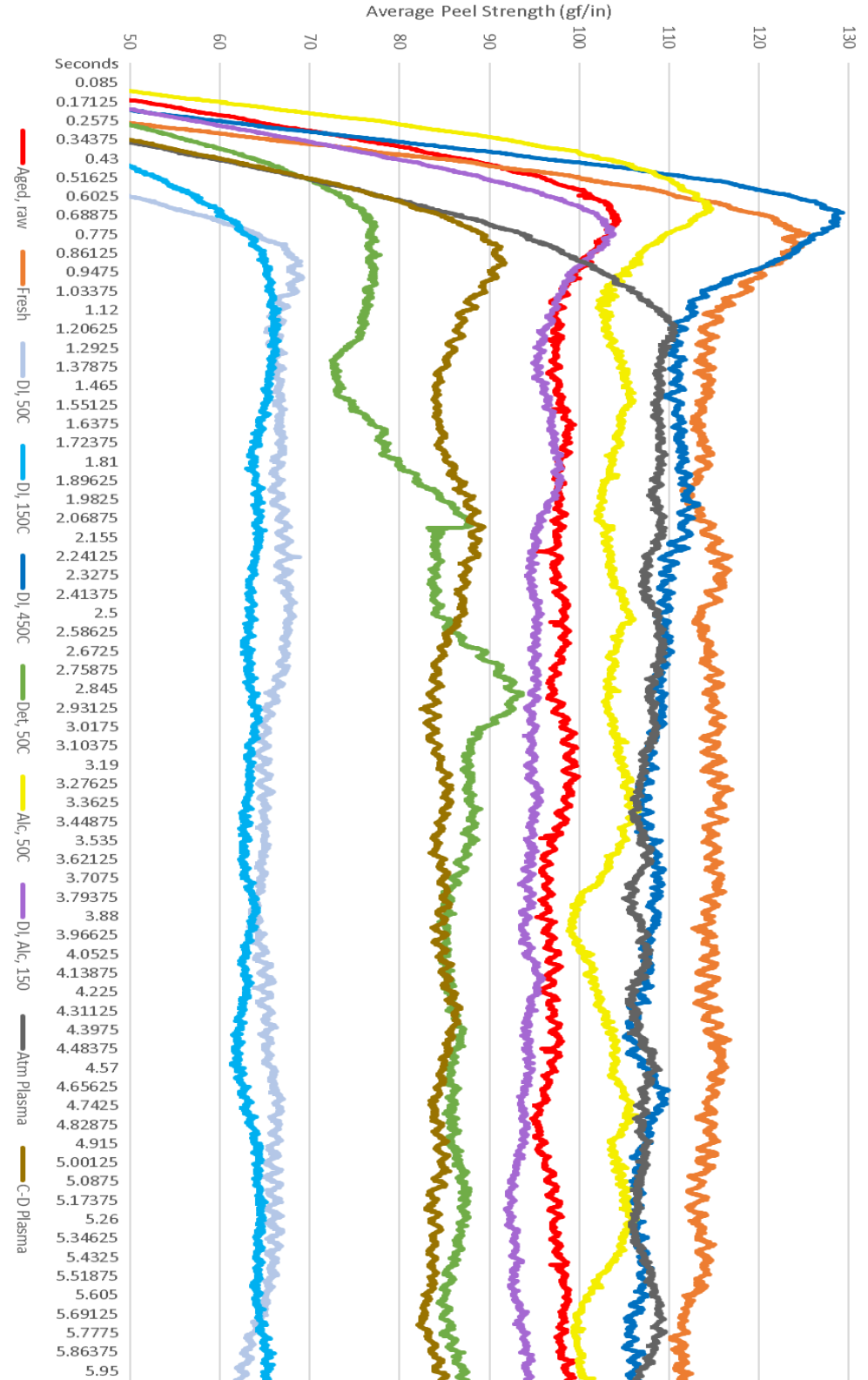
	Aged raw	Fresh	DI, 50C	DI, 150C	DI, 450C	Det, 50C	Alc, 50C	DI, Alc, 150	Atm Plasma	C-D Plasma
St. Dev	0.3761886	0.5915217	0.20585781	0.69620052	0.42054917	0.4764496	0.2973076	0.44472671	0.32829382	0.44120979
Trim Mean	9.55525407	10.4818513	12.1266416	16.9015572	7.38647423	10.528329	9.74638049	7.28907762	11.6675703	12.5868635
Coef. Var.	0.03936982	0.05643294	0.01697567	0.0411915	0.05693503	0.04525406	0.03050441	0.06101276	0.02813729	0.0350532

Cling Film, 180° Peel, 12"/min, Various Conditions



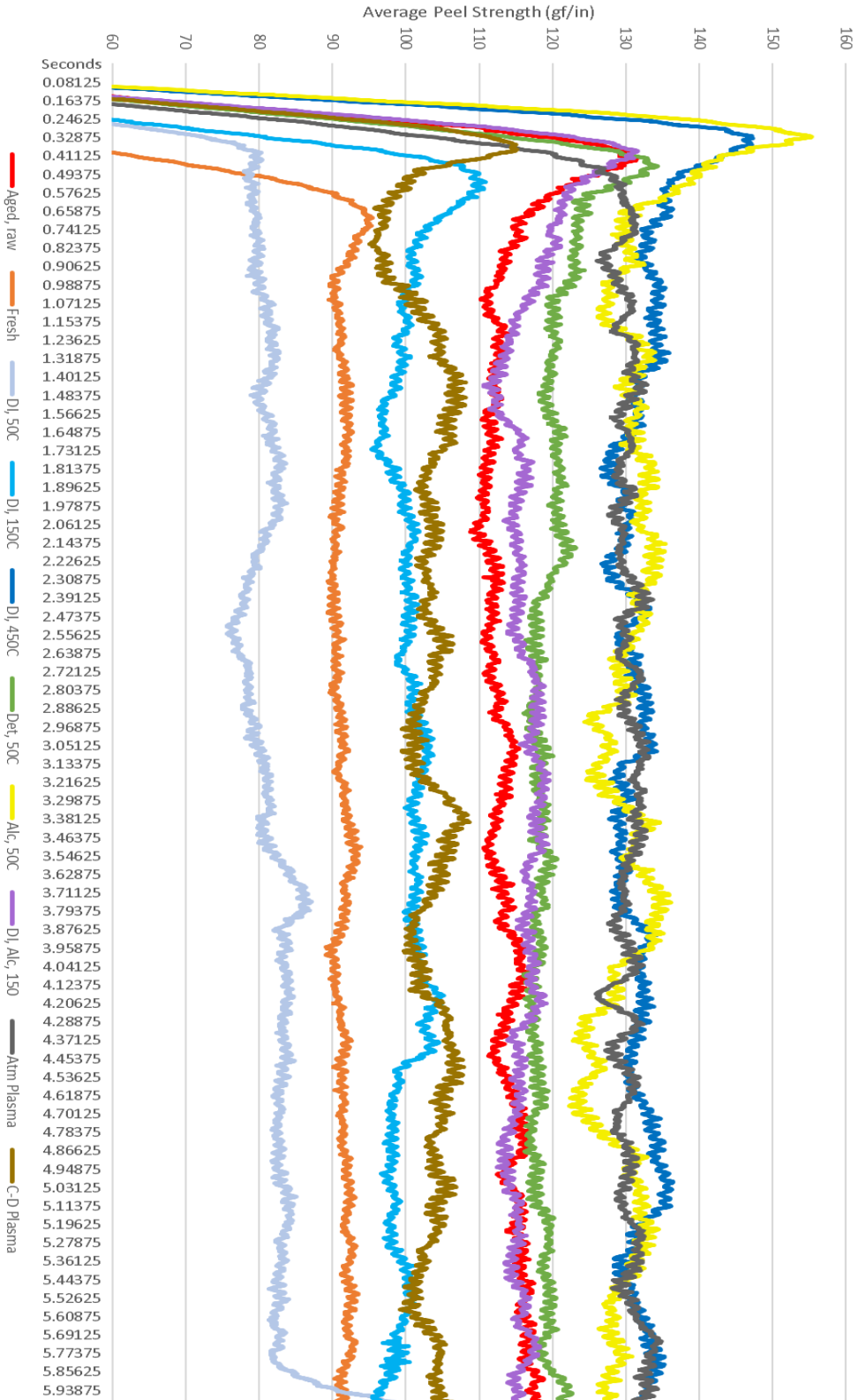
	Aged, raw	Fresh	D1, 50C	D1, 150C	D1, 450C	Det, 50C	A1c, 50C	D1, A1c, 150	Atm Plasma	C-D Plasma
St. Dev	0.65547835	0.35284143	0.25276161	0.60107124	0.47002918	0.37456897	0.60453811	0.85758656	0.34514805	0.42683142
Trim Mean	12.7017781	10.4543388	14.4412446	13.7405962	8.95912443	12.0843661	12.6168527	8.27337698	15.3377624	14.7687795
Coef. Var.	0.05160524	0.03375072	0.01750276	0.04374419	0.05246374	0.03099616	0.04791513	0.10365617	0.02250316	0.02890093

Frisket Film, 90° Peel, 3"/min, Various Conditions



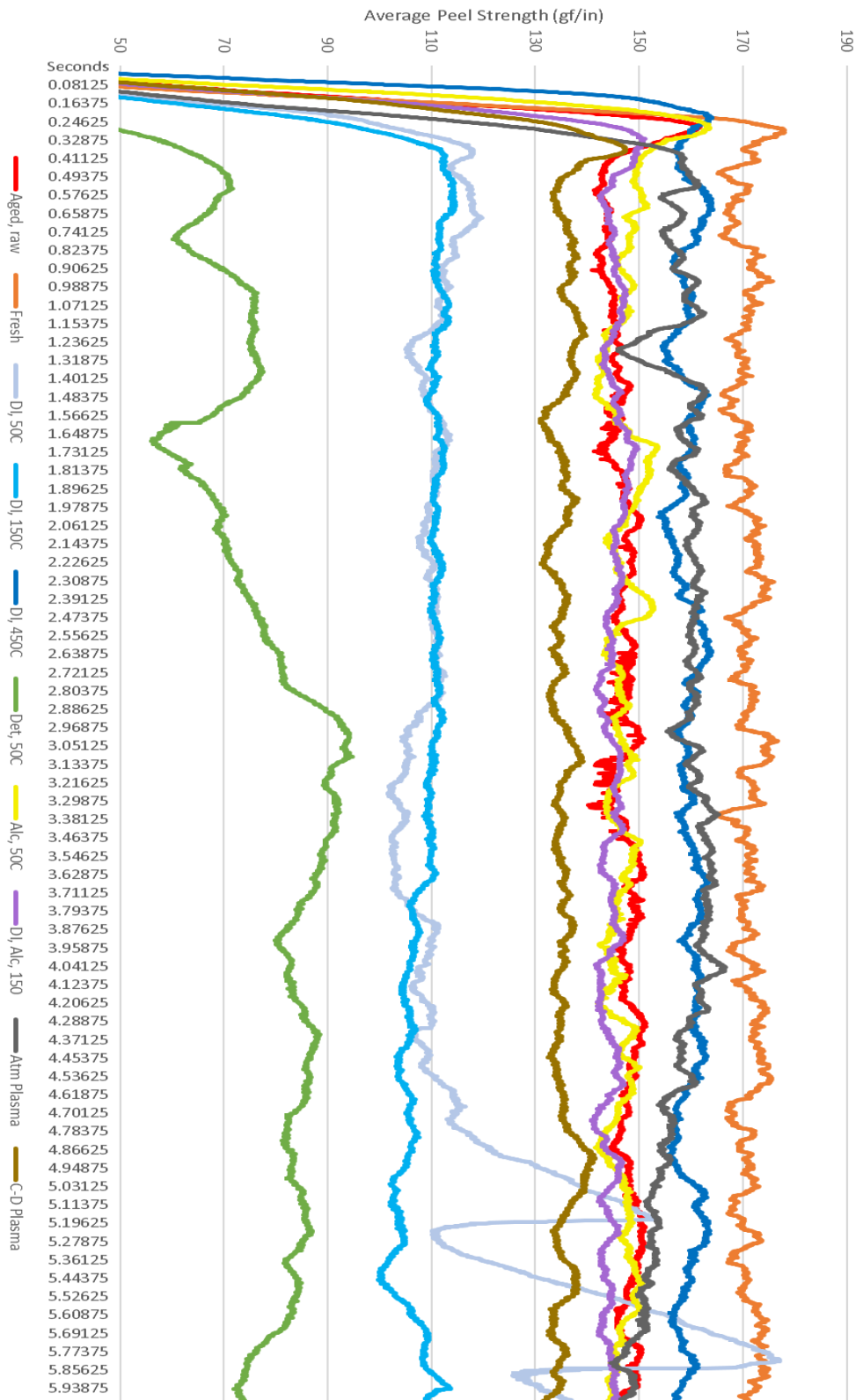
	Aged, raw	Fresh	DJ, 50C	DJ, 150C	DJ, 450C	Det, 50C	Alc, 50C	DJ, Alc, 150	Atm Plasma	C-D Plasma
St. Dev	0.96192569	1.22876066	1.19997426	0.84614026	1.83535128	3.21329274	1.8368079	1.27989124	1.01608782	1.3724354
Trim Mean	97.5305953	114.206642	65.7239689	63.6567244	108.247987	85.9258694	103.404054	94.5648365	107.609247	84.8515612
Coef. Var.	0.00986281	0.0107591	0.01825779	0.01329224	0.01695506	0.0373961	0.0177634	0.01353454	0.00944238	0.01617455

Frisket Film, 90° Peel, 6"/min, Various Conditions



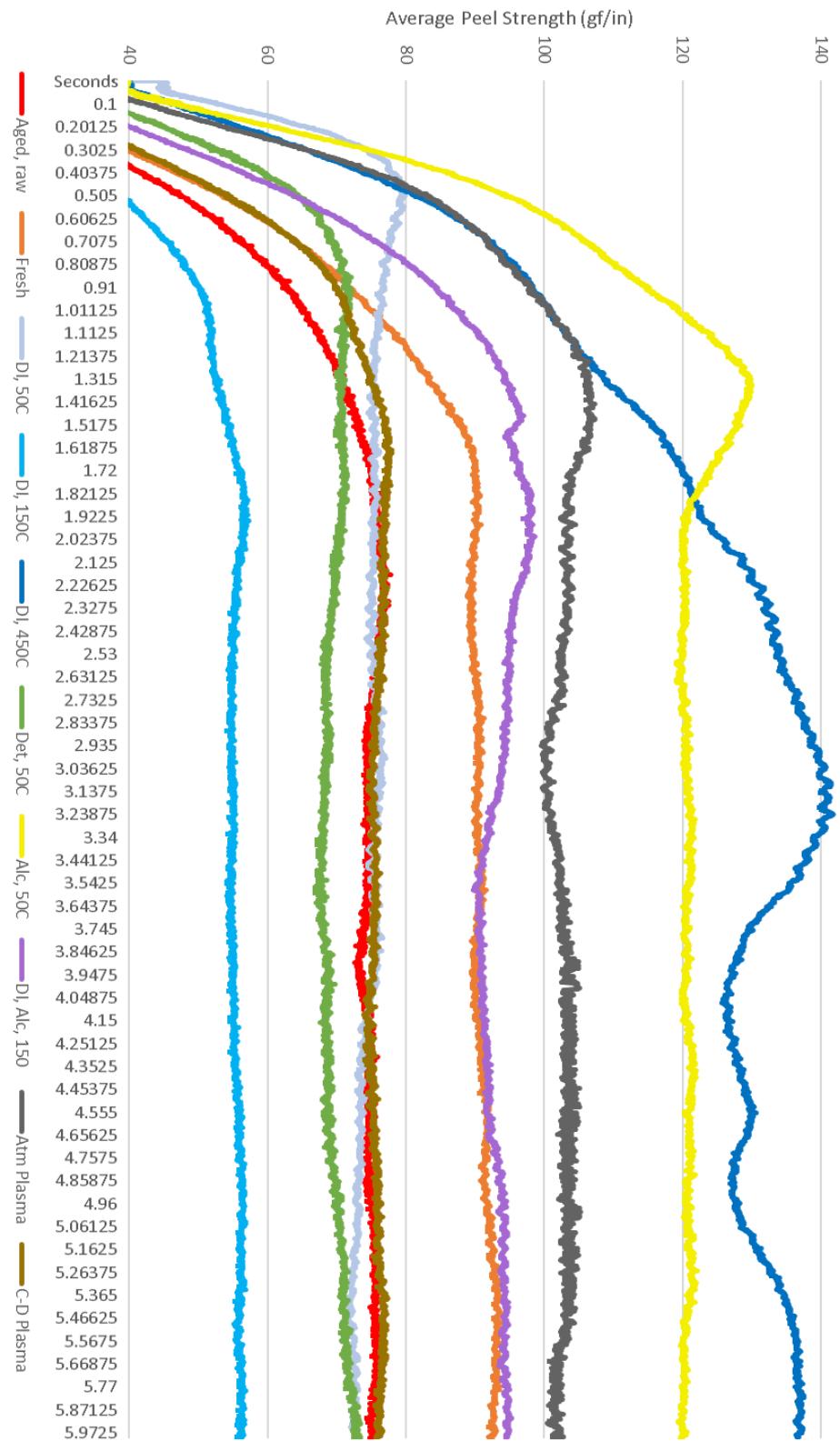
	Aged, raw	Fresh	DI, 50C	DI, 150C	DI, 450C	Det, 50C	Alc, 50C	DI, Alc, 150	Atm Plasma	C-D Plasma
St. Dev	2.06777761	0.85512017	2.72738731	1.95433882	1.98837069	1.4038649	2.99891145	1.51056692	1.46221205	1.82767504
Trim Mean	113.595149	91.3844296	81.9639889	100.048516	131.250321	118.702405	129.999464	115.995178	130.461054	103.715599
Coef. Var.	0.01820304	0.00935739	0.03327543	0.01953391	0.01514945	0.01182676	0.02306864	0.01302267	0.01120803	0.01762199

Frisket Film, 90° Peel, 12"/min, Variable Conditions



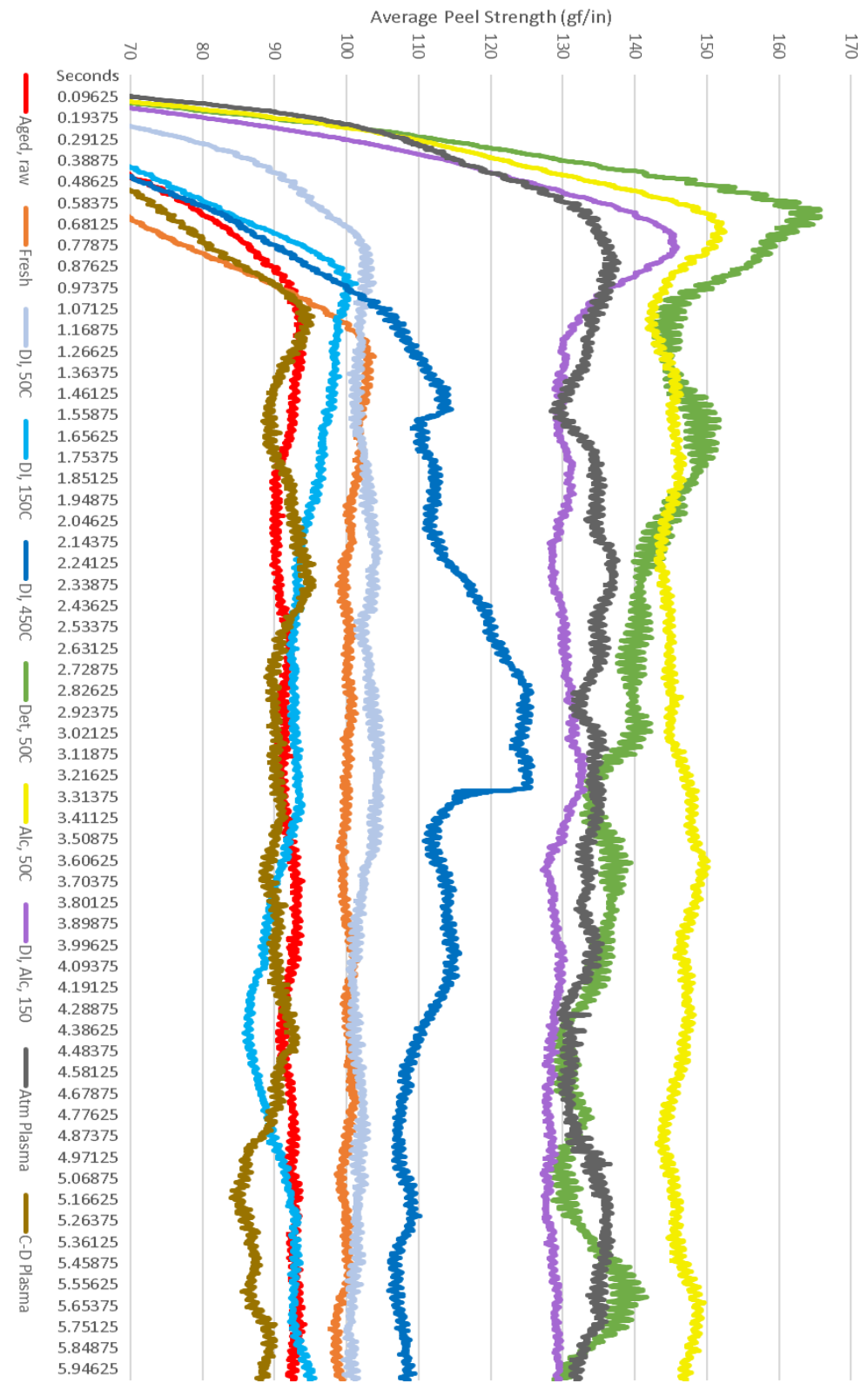
	Aged, raw	Fresh	DJ, 50C	DJ, 150C	DJ, 450C	Det, 50C	Aic, 50C	DJ, Aic, 150	Atm Plasma	C-D Plasma
St. Dev	1.87950458	2.08609403	16.4271	3.14289819	2.013849	8.43360222	2.37318389	1.66258623	4.69262416	1.82413542
Trim Mean	147.858379	171.222242	114.604705	108.233032	159.667734	81.5008755	146.830791	144.783056	158.452934	135.149251
Coef. Var.	0.01271152	0.01218355	0.14333705	0.02903825	0.01261275	0.10347867	0.01616271	0.01148329	0.02961526	0.01349719

Frisket Film, 180° Peel, 3"/min, Various Conditions



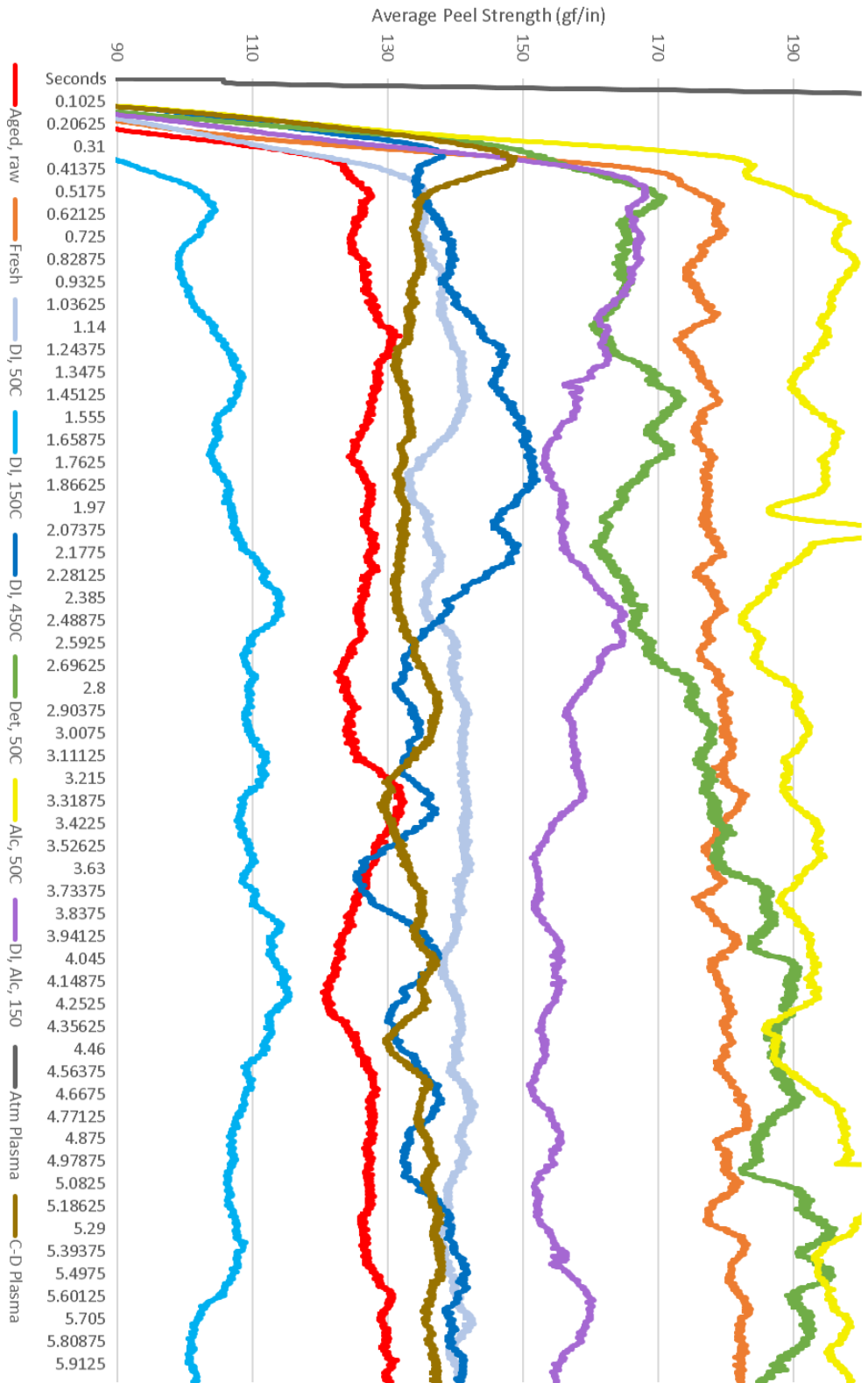
	Aged, raw	Fresh	DI, 50C	DI, 150C	DI, 450C	Det, 50C	Alc, 50C	DI, Alc, 150	Atm Plasma	C-D Plasma
St. Dev	0.87034508	1.23861516	1.39635473	0.67495114	5.91548656	1.38247833	1.37466508	2.07049097	1.25972274	0.78560225
Trim Mean	75.0488419	90.9204643	74.4905361	55.5079082	131.61476	69.5024429	120.752082	93.7279799	102.779607	75.9609402
Coef. Var.	0.01159705	0.01362306	0.0187454	0.01215955	0.04494546	0.01989108	0.01138419	0.02209043	0.01225654	0.01034219

Frisket Film, 180° Peel, 6"/min, Various Conditions



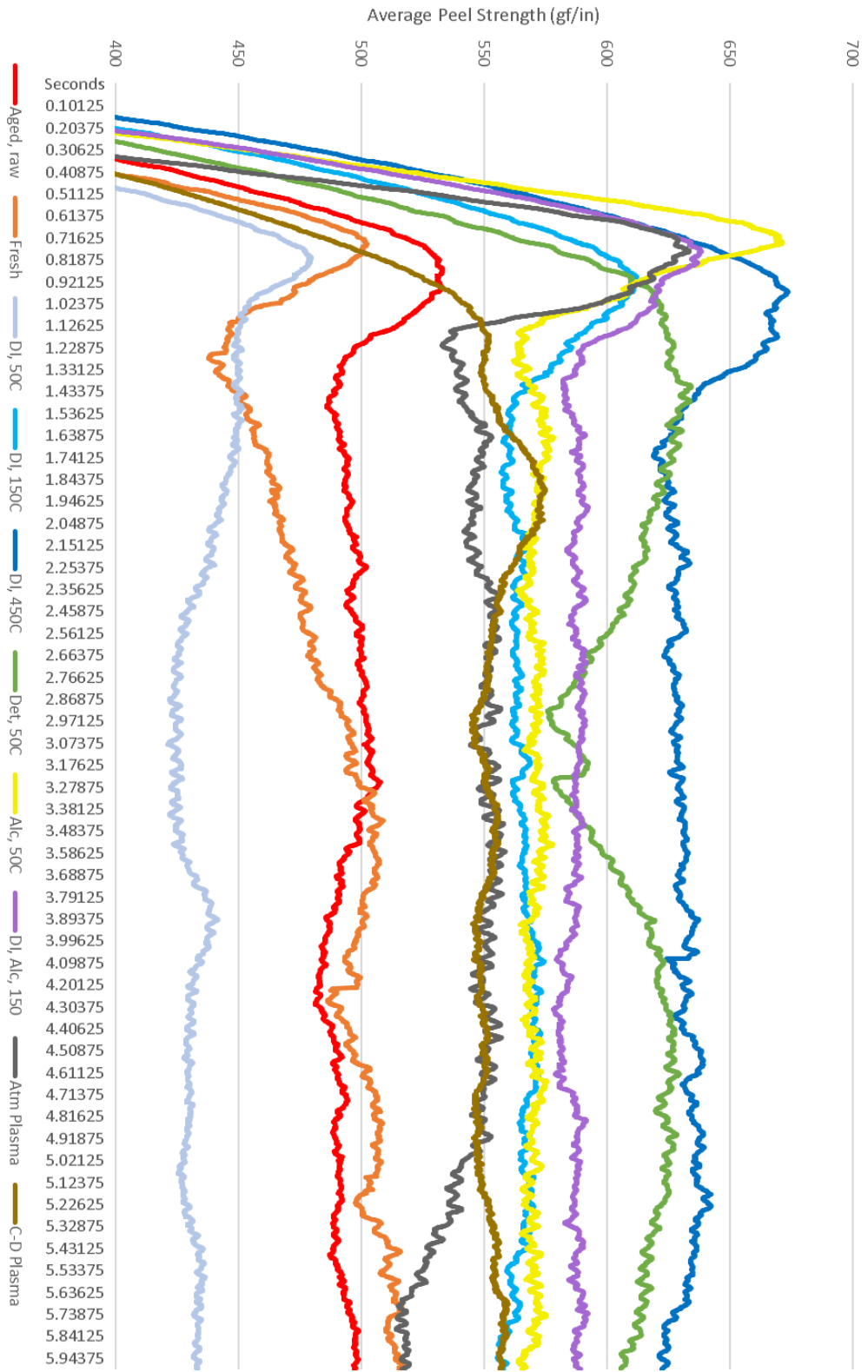
	Aged, raw	Fresh	DI, 50C	DI, 150C	DI, 450C	Det, 50C	Alc, 50C	DI, Alc, 150	Atm Plasma	C-D Plasma
St. Dev	0.98332338	0.82102395	1.22977951	2.76619947	5.61299584	5.49845321	1.57986142	1.26745909	1.85759875	2.20263586
Trim Mean	91.9463945	100.181142	102.28315	91.9877318	112.957084	136.970602	146.172304	129.417898	133.822709	89.9845875
Coef. Var.	0.01069453	0.00819539	0.01202329	0.0300714	0.0496914	0.04014331	0.01080821	0.00979354	0.01388104	0.02447792

Frisket Film, 180° Peel, 12"/min, Various Conditions



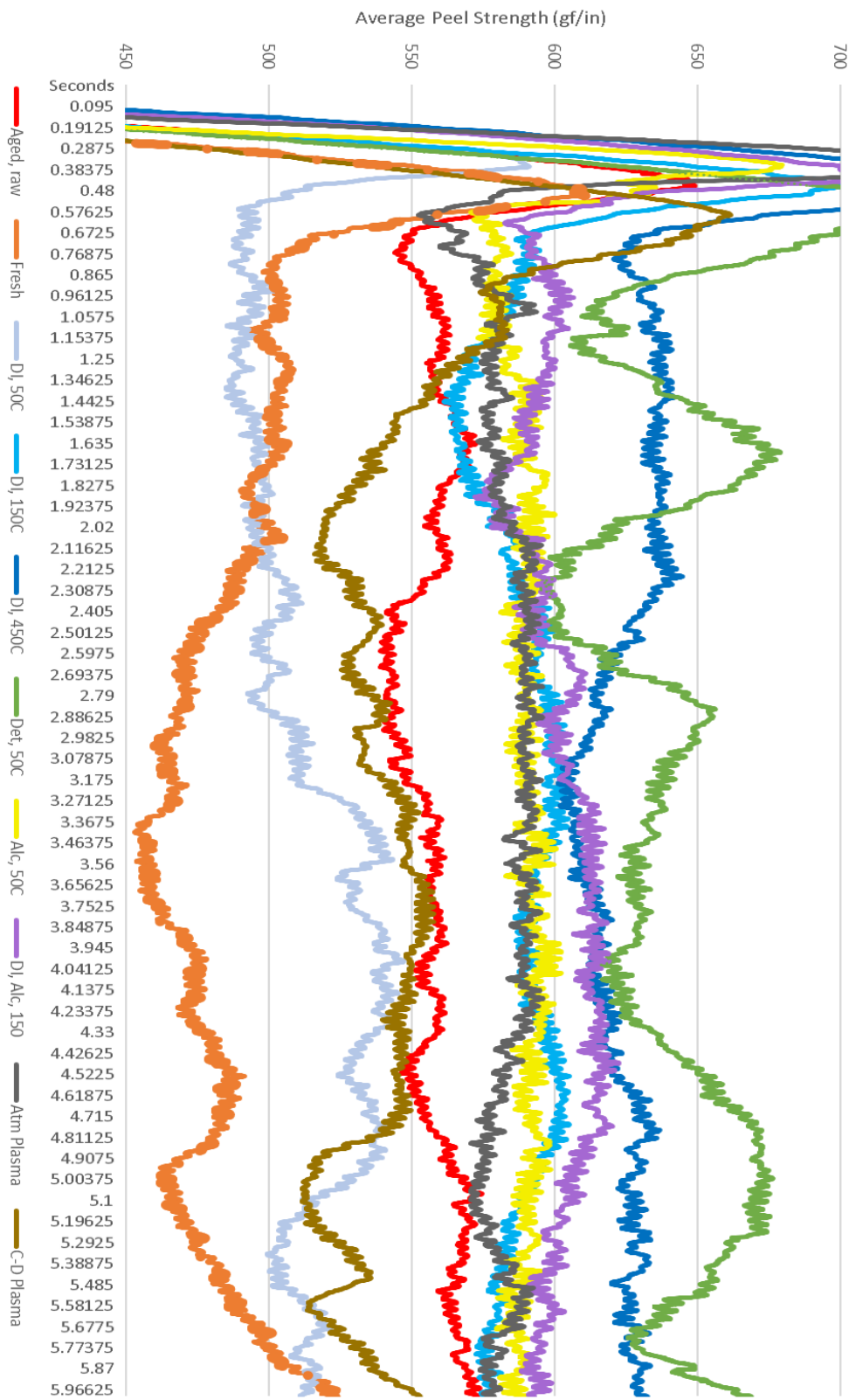
	Aged, raw	Fresh	DI, 50C	DI, 150C	DI, 450C	Det, 50C	Alc, 50C	DI, Alc, 150	Atm Plasma	C-D Plasma
St. Dev	2.40967055	2.01064207	2.18155867	3.4098513	6.43544067	9.98897622	4.78182568	3.23563384	8.99071949	2.31426658
Trim Mean	126.716967	179.519933	139.672867	108.834301	137.485233	180.649323	192.6958	155.799928	429.433502	134.328623
Coef. Var.	0.01901616	0.0112001	0.01561906	0.03133067	0.04680823	0.05529484	0.02481541	0.02076788	0.02093623	0.0172284

Blue Tape, 90° Peel, 3"/min, Various Conditions



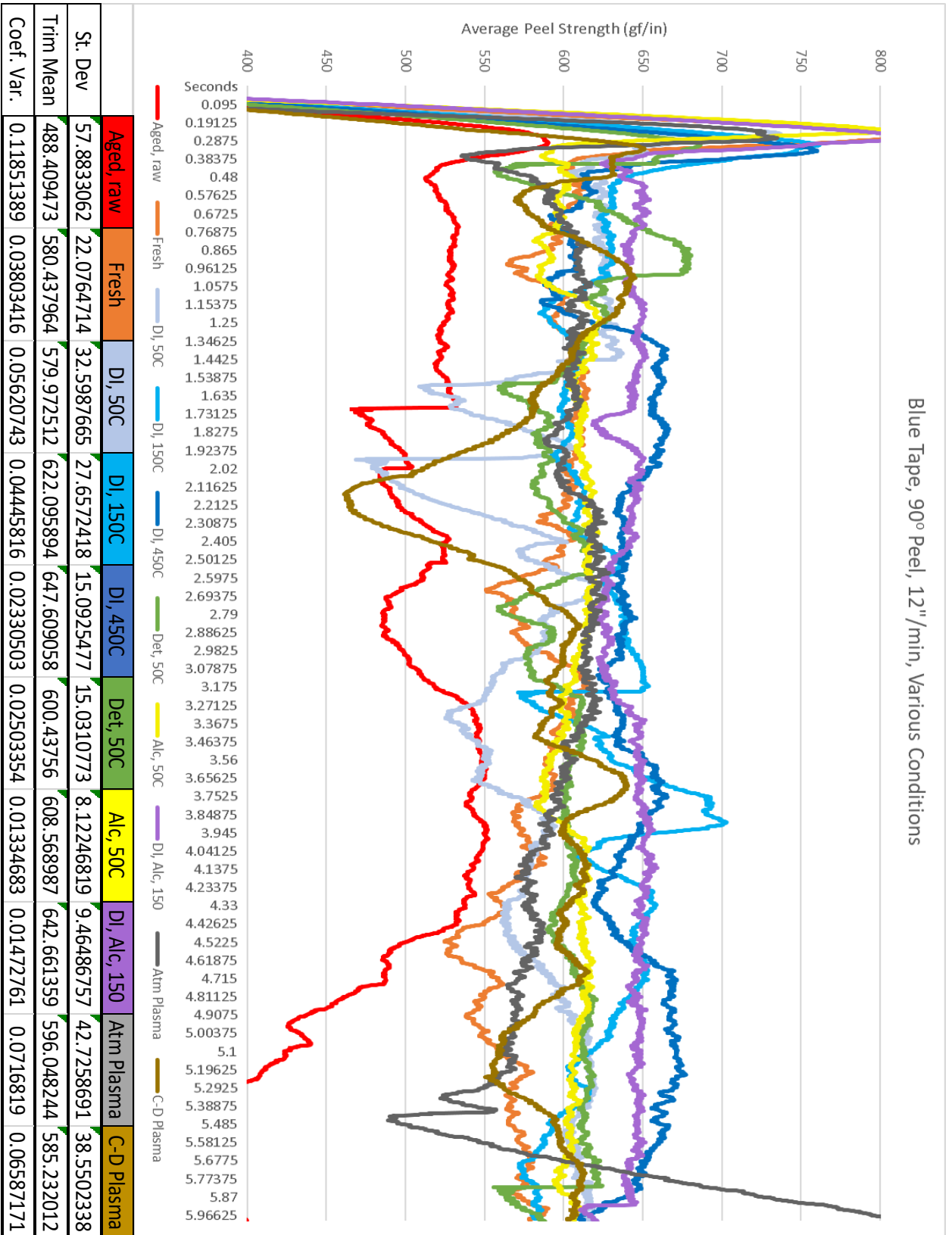
	Aged, raw	Fresh	DI, 50C	DI, 150C	DI, 450C	Det, 50C	Alc, 50C	DI, Alc, 150	Atm Plasma	C-D Plasma
St. Dev	5.67005028	16.8394037	6.90702352	3.94126009	4.60467005	14.7233405	2.58214906	2.87452651	10.9791756	7.08413598
Trim Mean	493.802415	493.690484	431.993947	565.047725	630.631921	612.214839	570.624079	587.156345	546.305269	553.522103
Coef. Var.	0.01148243	0.03410923	0.0159887	0.00697509	0.00730168	0.0240493	0.00452513	0.00489567	0.02009714	0.01279829

Blue Tape, 90° Peel, 6"/min, Various Conditions

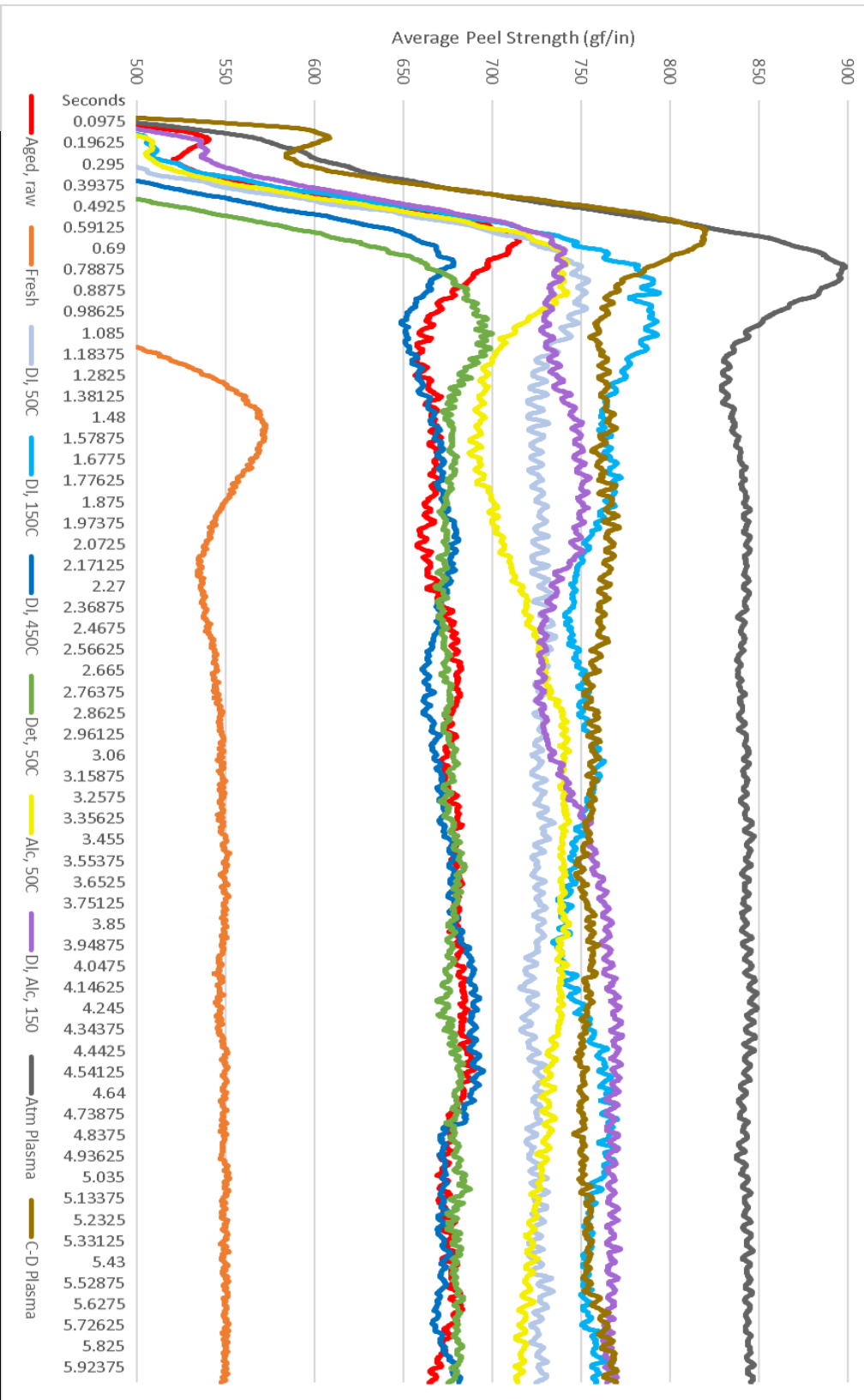


	Aged, raw	Fresh	DI, 50C	DI, 150C	DI, 450C	Det, 50C	Alc, 50C	DI, Alc, 150	Atm Plasma	C-D Plasma
St. Dev	8.65617426	14.9984791	16.3107346	10.1536846	10.0240971	21.2212847	4.02030113	10.6925001	6.29550755	12.0521051
Trim Mean	558.01591	478.906736	516.766518	589.844666	623.566773	641.258552	591.090636	603.372757	585.170715	536.242969
Coef. Var.	0.01551241	0.03131816	0.03156306	0.01721417	0.01607542	0.03309318	0.0068015	0.01772122	0.01075841	0.02247508

Blue Tape, 90° Peel, 12"/min, Various Conditions

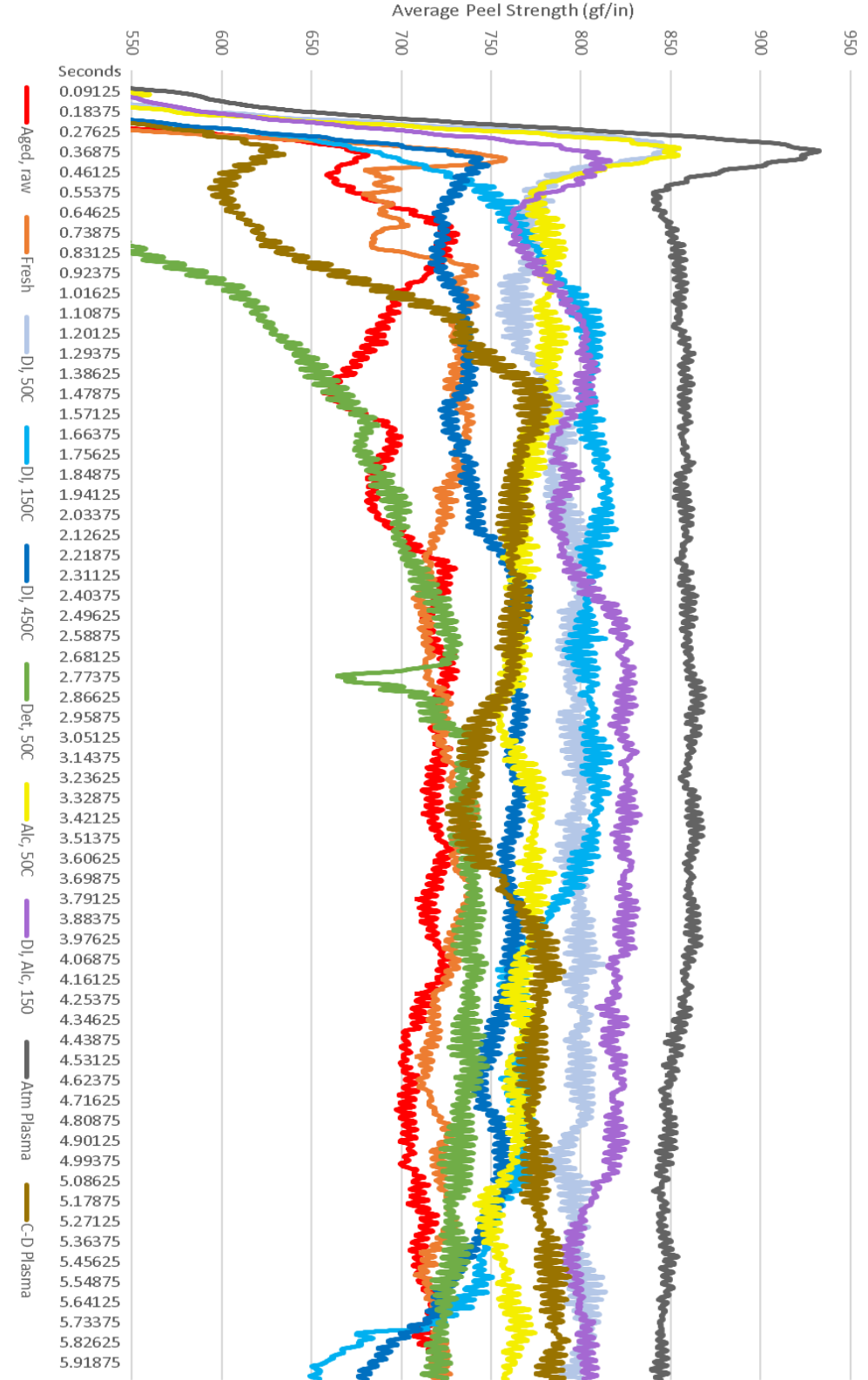


Blue Tape, 180° Peel, 3"/min, Various Conditions



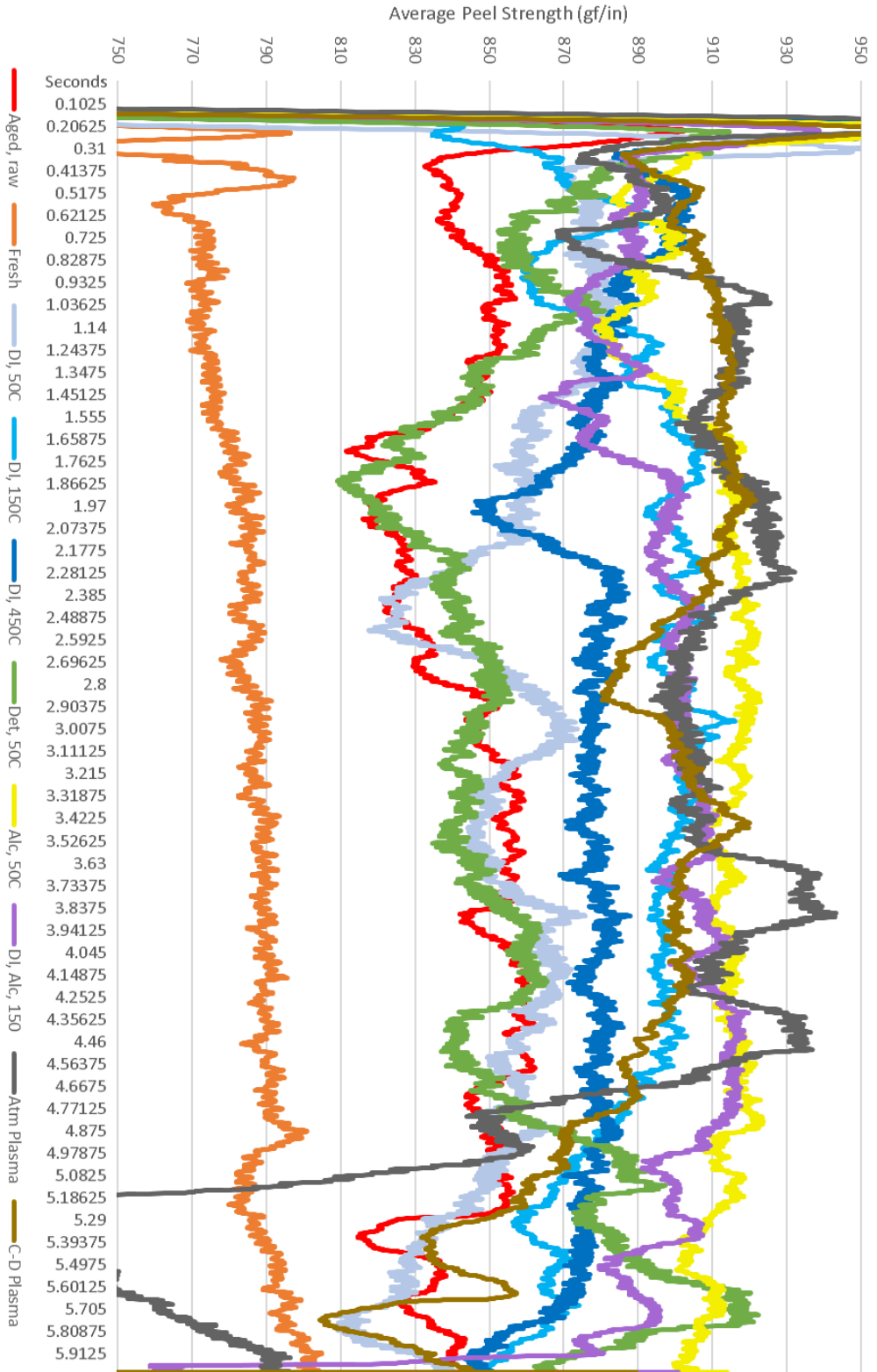
	Aged, raw	Fresh	DI, 50C	DI, 150C	DI, 450C	Det, 50C	Alc, 50C	DI, Alc, 150	Atm Plasma	C-D Plasma
St. Dev	6.49929465	6.29505383	3.42116189	8.3599893	7.75464416	3.48576805	14.5622362	14.7230208	2.33950312	5.62767446
Trim Mean	676.155396	548.012186	726.137436	754.280685	675.222508	677.406514	726.851646	755.47665	842.774651	756.925772
Coef. Var.	0.00961213	0.01148707	0.00471145	0.01108339	0.01148458	0.00514576	0.02003467	0.01948839	0.00277595	0.00743491

Blue Tape, 180° Peel, 6"/min, Various Conditions



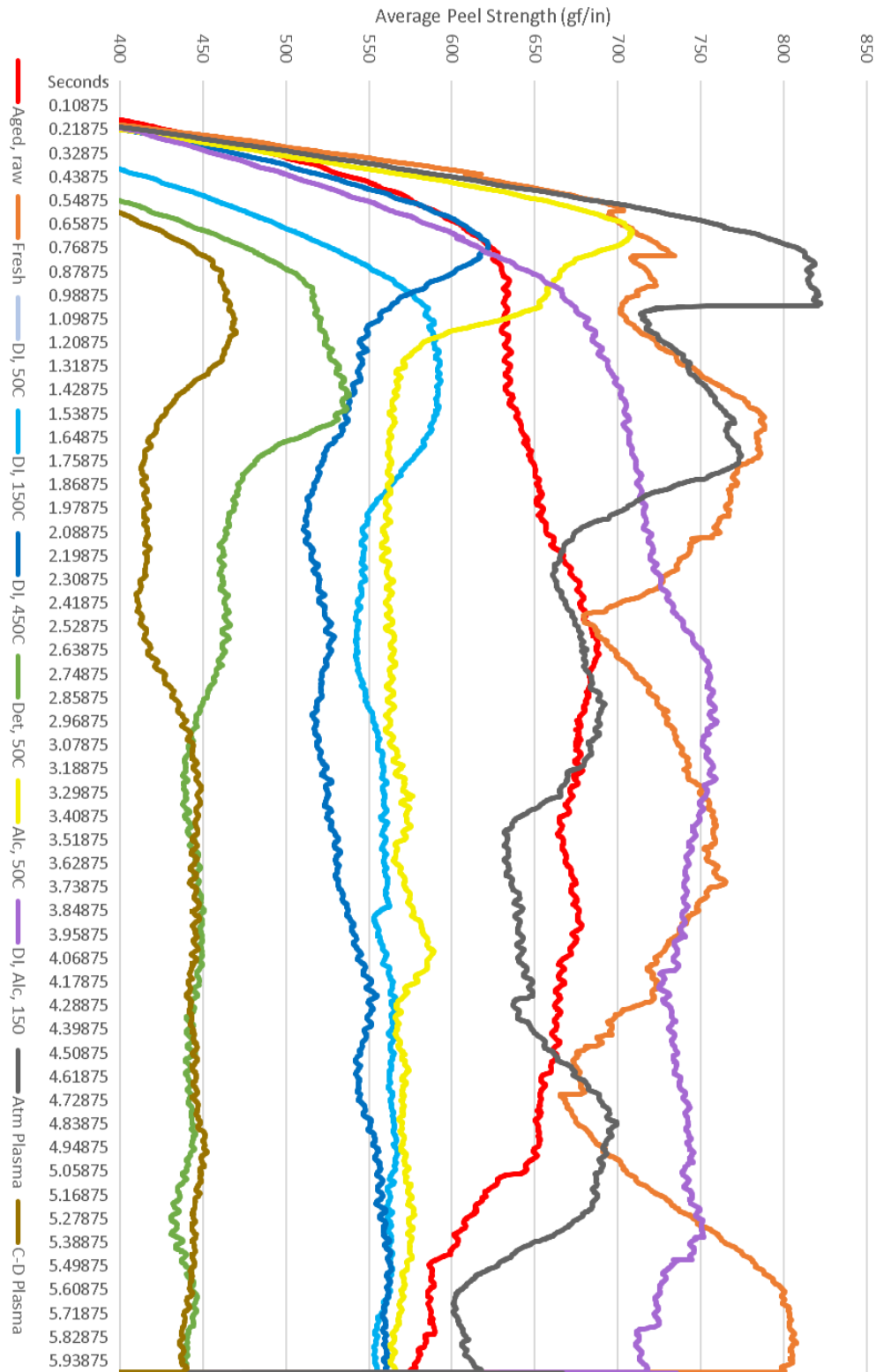
	Aged, raw	Fresh	DJ, 50C	DJ, 150C	DJ, 450C	Det, 50C	Aic, 50C	DJ, Aic, 150	Atm Plasma	C-D Plasma
St. Dev	12.2960386	7.9421619	6.60771313	36.0207656	19.2872774	19.1873315	8.14421188	13.8211493	6.77855481	14.9420637
Trim Mean	711.889107	723.256626	796.927115	782.640676	751.011628	724.044806	765.45581	812.041372	855.53152	767.155002
Coef. Var.	0.01727241	0.01098111	0.00829149	0.04602465	0.02568173	0.0265002	0.01063969	0.01702025	0.00792321	0.01947724

Blue Tape, 180° Peel, 12"/min, Various Conditions



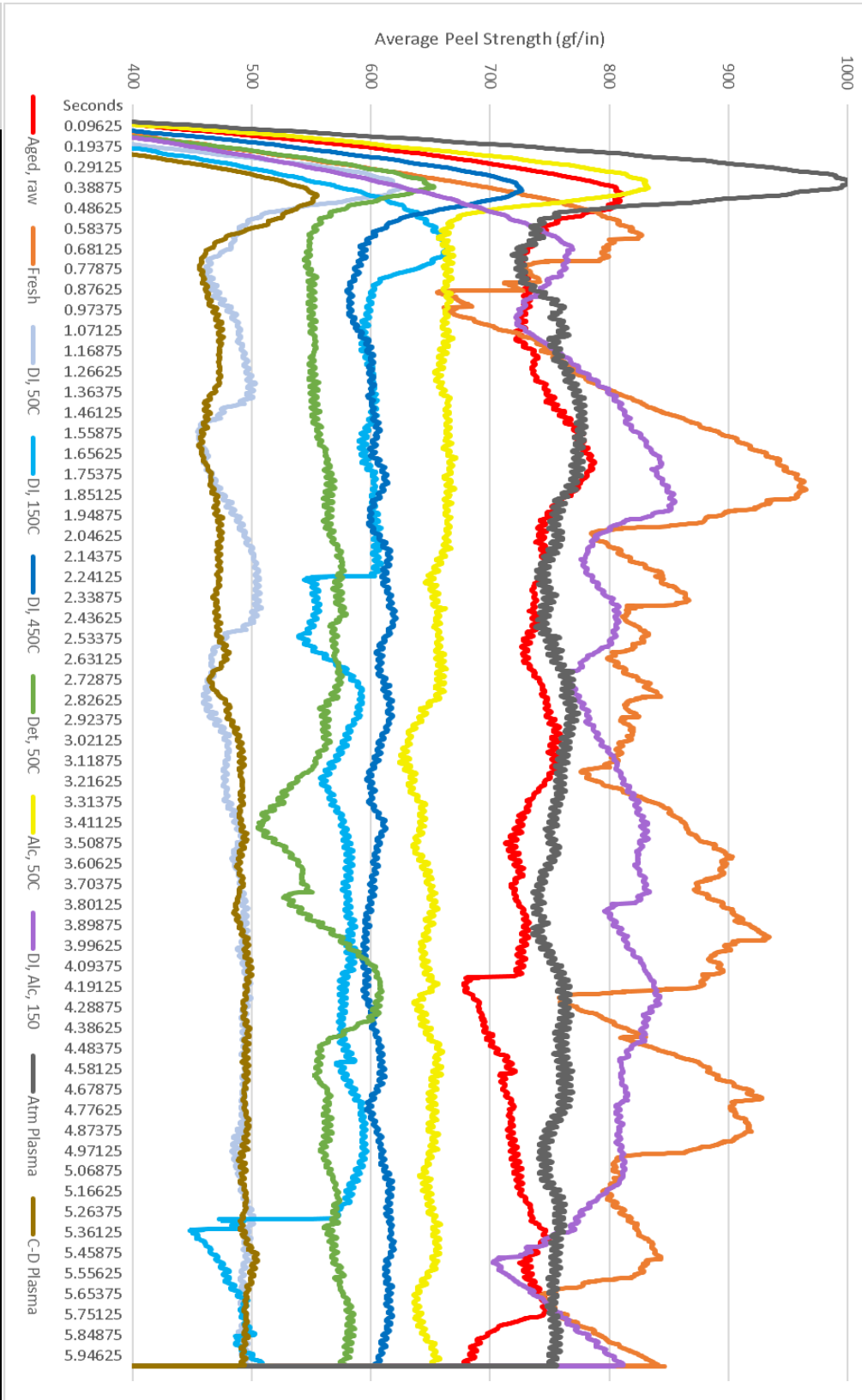
	Aged, raw	Fresh	D1, 50C	D1, 150C	D1, 450C	Det, 50C	Alc, 50C	D1, Alc, 150	Atm Plasma	C-D Plasma
St. Dev	13.6097519	5.18276943	15.0177016	15.7120349	8.76326671	23.592695	5.12464289	16.802214	67.4884555	28.1616908
Trim Mean	842.743273	787.942285	850.534136	891.870718	875.57495	853.561159	914.047884	900.782263	882.053527	889.559272
Coef. Var.	0.01614935	0.0065776	0.01765679	0.01761694	0.01000859	0.02764031	0.00560654	0.01865291	0.07651288	0.03165803

Red Tape, 90° Peel, 3"/min, Various Conditions



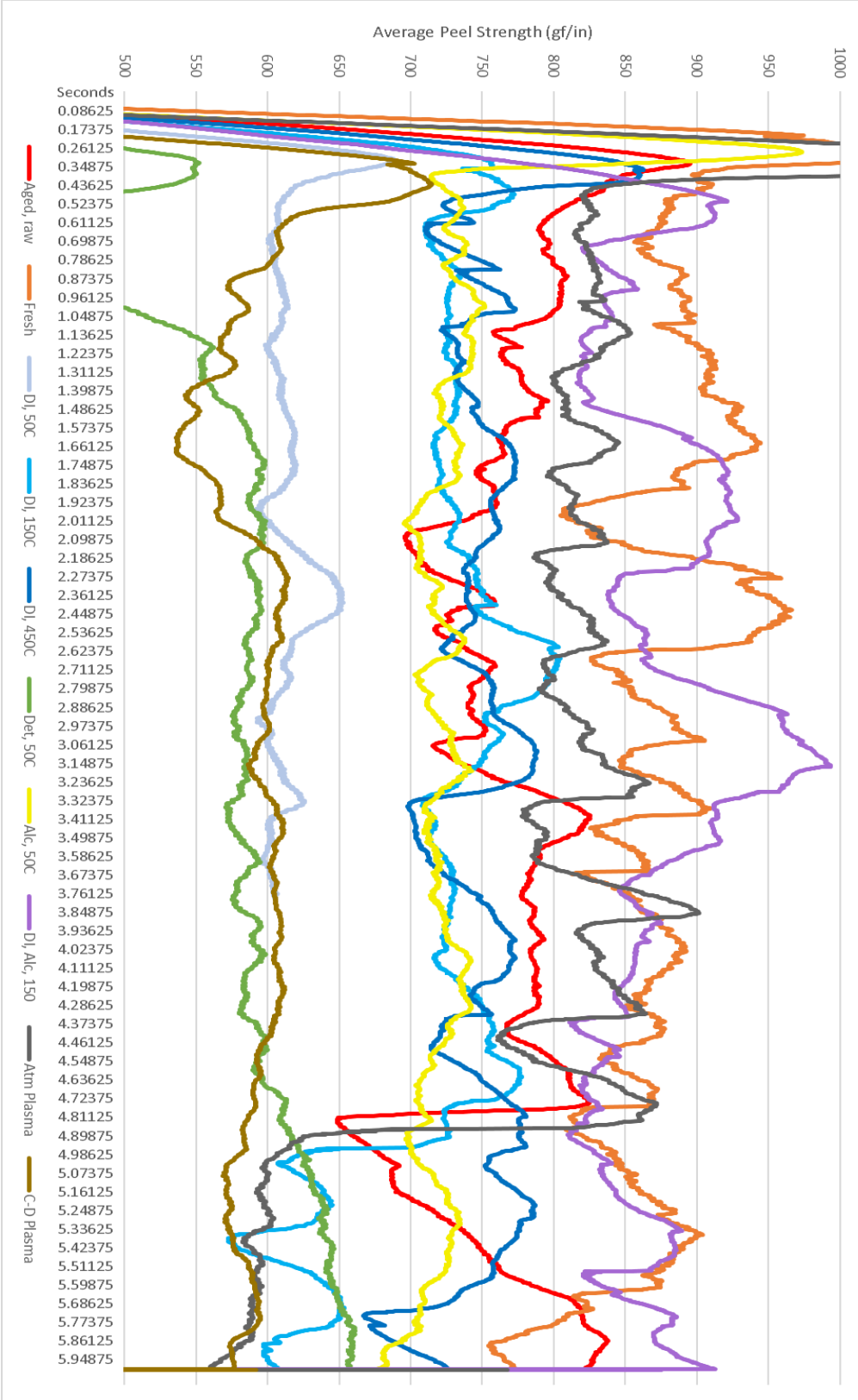
	Aged, raw	Fresh	DI, 50C	DI, 150C	DI, 450C	Det, 50C	Alc, 50C	DI, Alc, 150	Atm Plasma	C-D Plasma
St. Dev	30.8181657	37.9421922	#DIV/0!	9.77818589	16.1753768	18.726917	6.29648732	14.5519816	39.9585449	12.91873
Trim Mean	653.644248	738.422776	#NUM!	558.443082	537.464007	449.348015	568.190145	735.576965	666.922527	436.676068
Coef. Var.	0.04714822	0.05138275	#DIV/0!	0.01750973	0.03009574	0.04167575	0.01108166	0.01978308	0.05991482	0.02958424

Red Tape, 90° Peel, 6"/min, Various Conditions



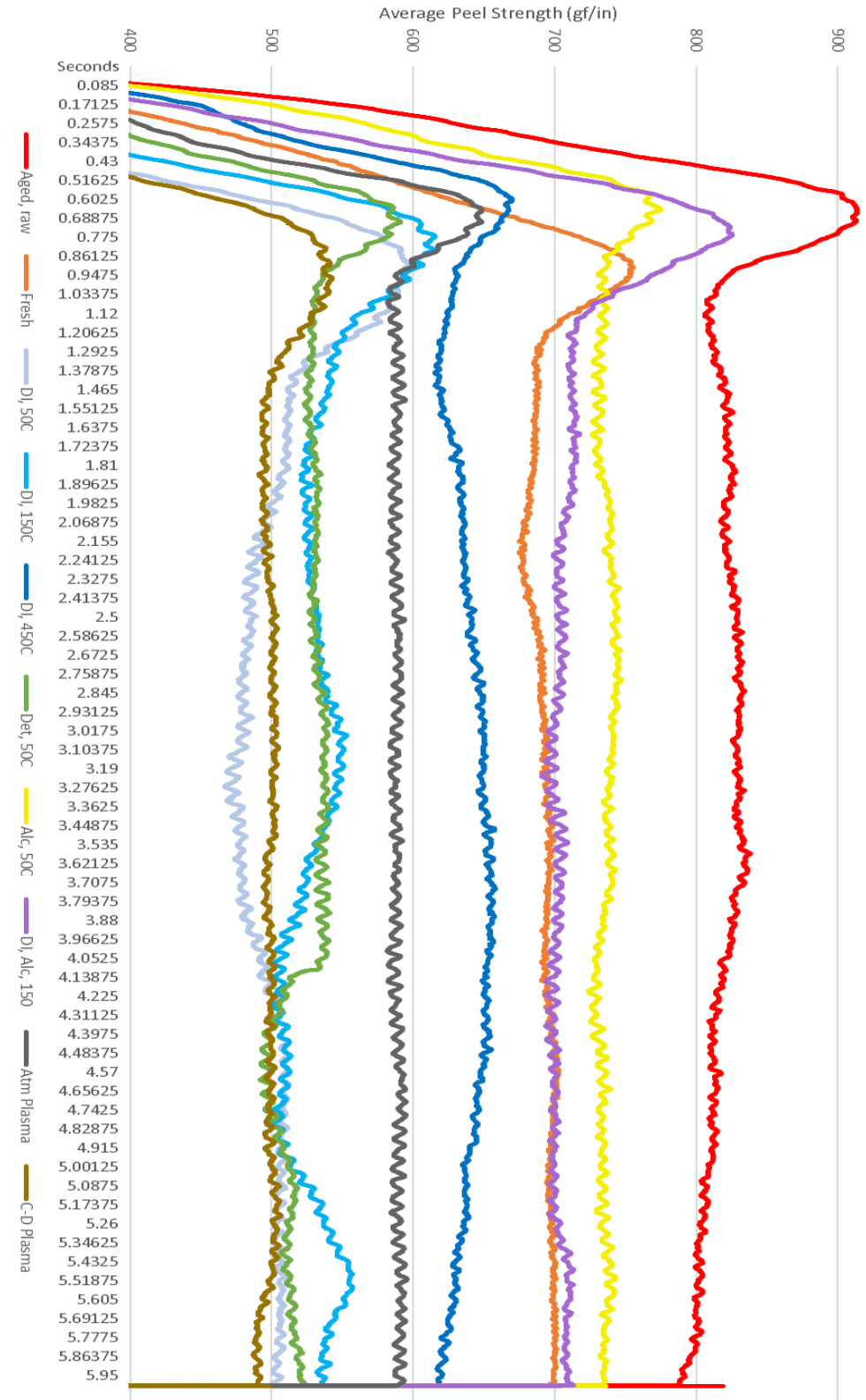
	Aged, raw	Fresh	D1, 50C	D1, 150C	D1, 450C	Det, 50C	Alc, 50C	D1, Alc, 150	Atm Plasma	C-D Plasma
St. Dev	22.3224522	50.934757	12.2101596	38.4520156	6.84074594	19.4840167	9.31594422	30.3443971	9.01855644	11.9033615
Trim Mean	731.686394	847.115184	487.489469	569.739233	607.482132	564.976829	650.381577	804.361016	755.924346	486.553145
Coef. Var.	0.03050822	0.06012731	0.02504702	0.06749055	0.01126082	0.0344864	0.01432381	0.03772485	0.0119305	0.02446467

Red Tape, 90° Peel, 12"/min, Various Conditions



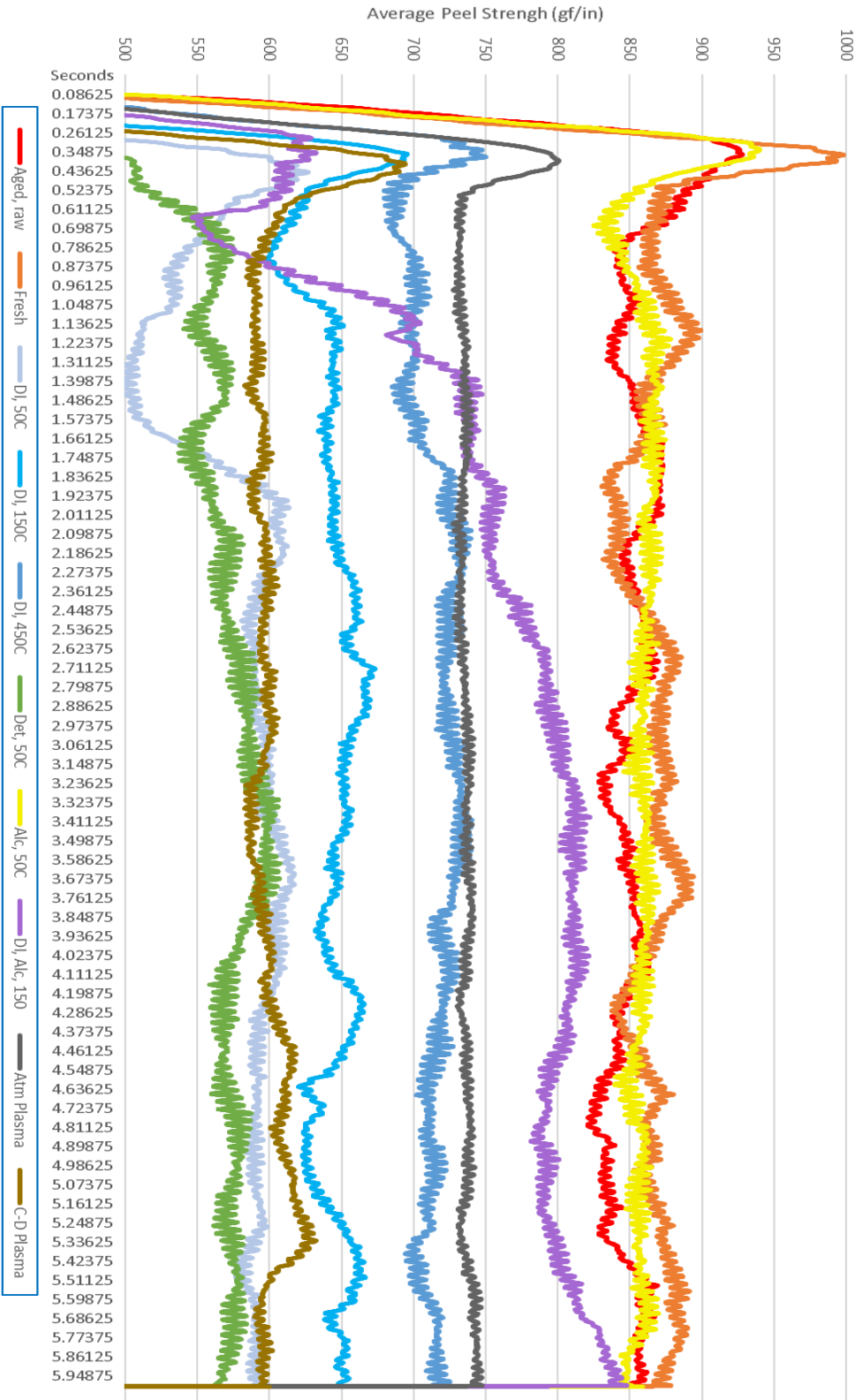
	Aged, raw	Fresh	DI, 50C	DI, 150C	DI, 450C	Det, 50C	Alc, 50C	DI, Alc, 150	Atm Plasma	C-D Plasma
St. Dev	42.4556834	42.0303356	14.714264	55.5949452	26.1824418	24.9192969	12.8968788	42.7464467	100.807853	18.4037286
Trim Mean	761.808592	866.781446	613.364331	716.644034	749.754765	600.508529	718.728395	875.443128	767.719476	592.317604
Coef. Var.	0.05573012	0.04849012	0.02398944	0.07757679	0.03492134	0.04149699	0.01794402	0.04882835	0.13130819	0.03107071

Red Tape, 180° Peel, 3"/min, Various Conditions



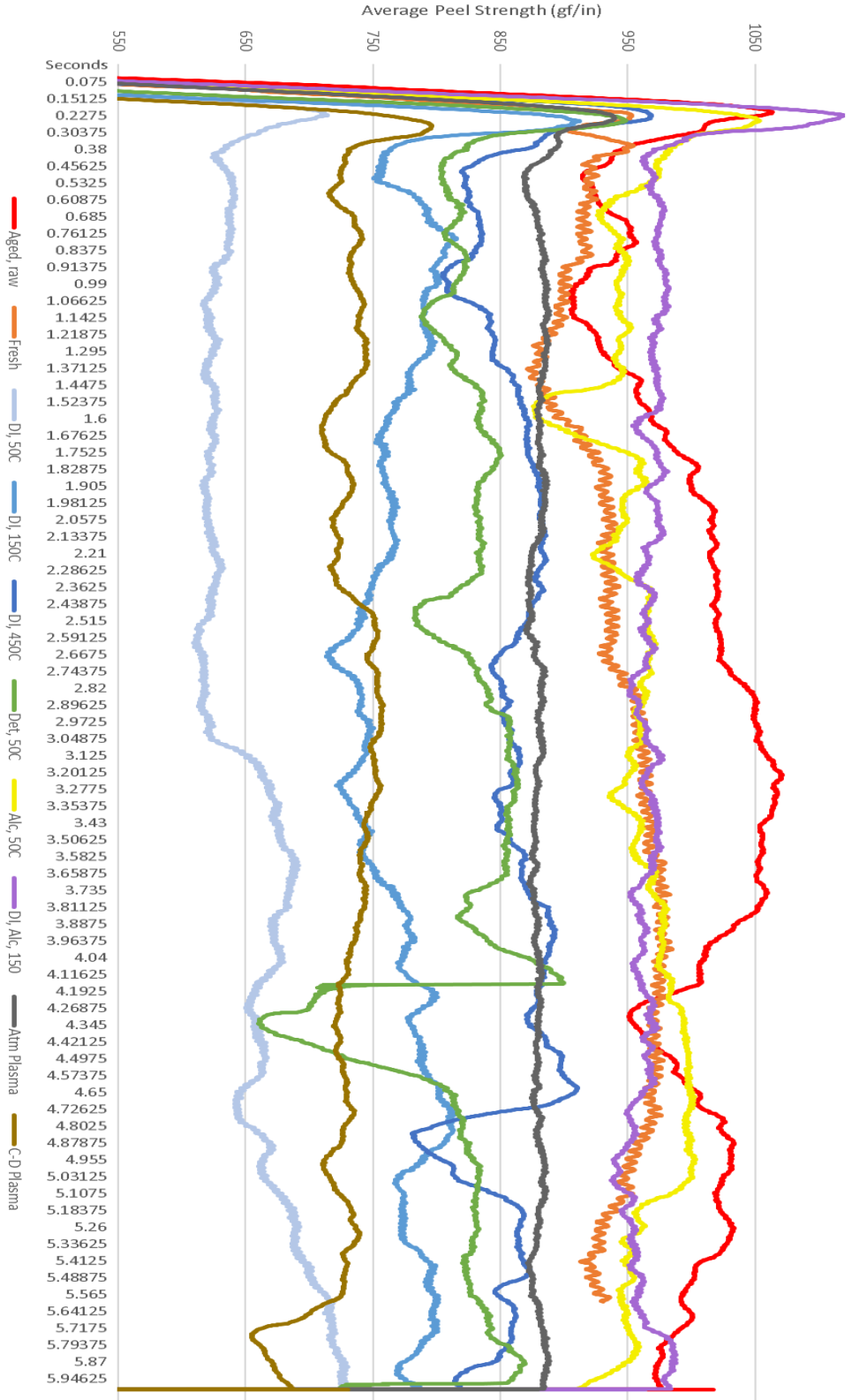
	Aged, raw	Fresh	DI, 50C	DI, 150C	DI, 450C	Det, 50C	Alc, 50C	DI, Alc, 150	Atm Plasma	C-D Plasma
St. Dev	11.3939342	6.69342931	13.1773706	14.6056482	10.5121736	13.3921418	4.68948666	5.25452394	2.7866376	3.73923914
Trim Mean	819.094224	693.541493	495.730402	528.425184	641.72829	523.982902	736.577109	703.755788	588.873551	498.737735
Coef. Var.	0.01391041	0.00965109	0.02658173	0.02763995	0.01638104	0.02555836	0.00636659	0.0074664	0.00473215	0.00749741

Red Tape, 180° Peel, 6"/min, Various Conditions



	Aged, raw	Fresh	DJ, 50C	DJ, 150C	DJ, 450C	Det, 50C	Alc, 50C	DJ, Alc, 150	Atm Plasma	C-D Plasma
St. Dev	12.3678791	14.3426879	18.9883867	11.1574833	10.0933183	13.0921016	5.94978698	25.350443	3.62033087	9.71748463
Trim Mean	849.500165	865.656752	593.843149	648.389167	719.712515	575.409684	859.078338	793.112444	736.663487	599.726362
Coef. Var.	0.01455901	0.01656856	0.03197542	0.017208	0.0140241	0.02275266	0.00692578	0.03196324	0.0049145	0.0162032

Red Tape, 180° Peel, 12"/min, Various Conditions



	Aged, raw	Fresh	DI, 50C	DI, 150C	DI, 450C	Det, 50C	Alc, 50C	DI, Alc, 150	Atm Plasma	C-D Plasma
St. Dev	29.5709724	21.8473273	32.9776968	23.4040533	23.8057158	44.0192324	25.354366	9.624696	3.6444471	20.8567299
Trim Mean	1017.1105	951.798889	657.244402	767.362128	865.64387	829.06412	963.876178	964.048617	879.741596	730.590941
Coef. Var.	0.02907351	0.02295372	0.0501757	0.03049936	0.02750059	0.05309509	0.02630459	0.00998362	0.00414263	0.02854775